SU-SEL-67-091

Polarization of Ionospherically Propagated Waves

by

M. R. Epstein

October 1967

Technical Report No. 143

Prepared under
Office of Naval Research Contract
Nonr-225(64), NR 038 019, and
Advanced Research Projects Agency ARPA Order 196-67

RADIOSCIENCE LABORATORY

STANFORD ELECTRONICS LABORATORIES

STANFORD UNIVERSITY • STANFORD, CALIFORNIA

Technical Report No. 139
Contract Nonr-225(64)
SU-SEL-67-026
"Computer Prediction of the Effects of HF Oblique-Path Polarization Rotation with Frequency"
By M. R. Epstein
February 1967

Stanford Electronics Laboratories
Stanford, California
19 December 1967

ERRATA

Corrected figures 7d, 8a,b, and 12a,b on pages 11, 12, and 16, respectively, of the above report are given below. Subject pages should be annotated accordingly.

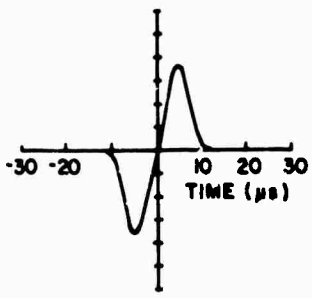

Fig. 7d

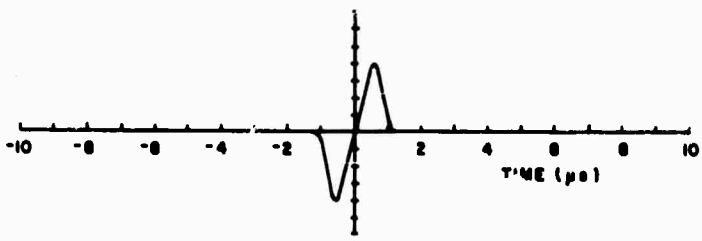

Fig. 12a

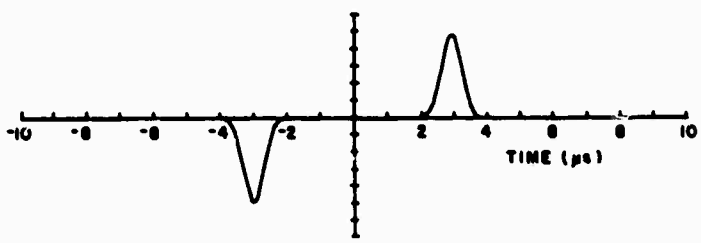

Fig. 12b

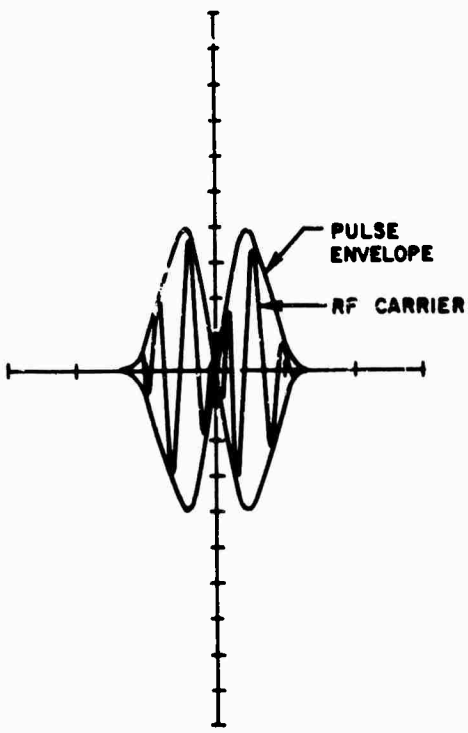

Fig. 8a

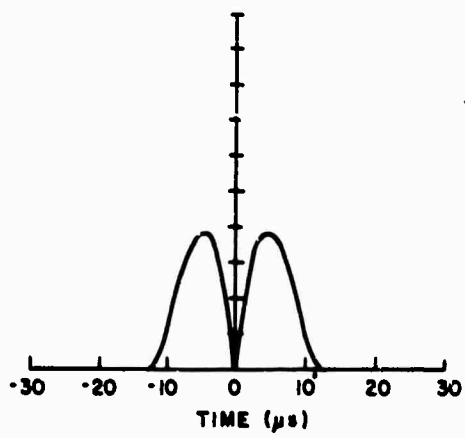

Fig. 8b

SEL-67-091

POLARIZATION OF IONOSPHERICALLY PROPAGATED WAVES

by

Mark R. Epstein

October 1967

Technical Report No. 143

Prepared under

Office of Naval Research Contract
Nonr-225(64), NR 088 019, and
Advanced Research Projects Agency
ARPA Order No. 196-67

Radioscience Laboratory
Stanford Electronics Laboratories
Stanford University Stanford, California

Contract Nonr-225(64), NR 088 019
October 1967

POLARIZATION OF IONOSPHERICALLY PROPAGATED WAVES

by
Mark R. Epstein

ABSTRACT

The theory of wave propagation in the ionosphere, supported by experimental measurements, is used to demonstrate that regular amplitude variations in HF sweep-frequency oblique-ionogram one-hop rays - when linearly polarized receiving antennas are employed - are due to corresponding variations of the received wave polarization with radio frequency. Over quasi-longitudinal paths the rate of occurrence of these variations with frequency (at some instant of time) was found (using computer raytracing techniques) to increase with increasing radio frequency and path length, and with increasingly close alignment of the propagation path with the longitudinal component of the earth's magnetic field. In addition, this rate is shown to be proportional to the group propagation-time difference between the two magnetoionic wave components at a given frequency. This relation explains certain remarkable features of the rate of occurrence of the variations.

Experimental measurements demonstrate that the position in the spectrum of the observed amplitude maxima moves with time in a manner consistent with individual-mode polarization rotation with time at a given frequency. An experimentally determined statistical description of this behavior is obtained for winter-noon conditions.

At some given time, amplitude variations of received signal strength as a function of frequency due to polarization rotation are shown to impose bandwidth limitations on pulsed or broadband skywave transmissions where waveform preservation is important. A measure of this limitation, expressed in terms of a coherent bandwidth, is proposed.

A model for the one-hop ionospheric signal channel is derived whose parameters are the rate of change of polarization rotation with frequency and the phase vs frequency characteristic of the path. These two parameters are shown to be readily determined from FM-CW or equivalent oblique-path sounding records. Using this model, predictions are made of the effects of polarization rotation with frequency, and also of ionospheric

dispersion or phase distortion, on the envelope shape of short-pulse signals. A pronounced waveshape distortion due to the effects of polarization rotation on the pulse envelope was observed when the signal bandwidth appreciably exceeded the "polarization bandwidth" for the path.

A method for skywave communication is proposed which involves polarization modulation and antennas that launch characteristically polarized waves. Experiment shows that this method possesses certain interesting properties not shared by other conventional modulation techniques.

It is proposed that the relation between magnetoionic group time and polarization be applied to FM-CW or equivalent oblique ionograms to determine the size of valleys in, and low-altitude values of, the electron density profile at midpath.

Polarization fluctuations of received ionospherically propagated waves are proposed as potentially useful indicators of the occurrence and location of ionospheric disturbances.

CONTENTS

CONTENTS (Continued)

ILLUSTRATIONS

ILLUSTRATIONS (Continued)

ACKNOWLEDGMENT

The author is grateful to Professor O. G. Villard, Jr. for his guidance and encouragement throughout the course of this work, and to Professor R. A. Helliwell and Dr. T. A. Croft for helpful discussions on several theoretical aspects of the research. The valuable help in computer programming, operation of transmitting equipment, and data reduction contributed by other members of the Radioscience Laboratory is acknowledged with appreciation.

BLANK PAGE

Chapter I

INTRODUCTION

The purpose of this research was to investigate the polarization of HF time-harmonic electromagnetic waves traveling over oblique-incidence ionospheric paths. Wave-polarization changes within the ionosphere are due to the presence of the earth's magnetic field. These changes, sometimes called Faraday rotation, were first observed in 1830 [1] when polarized light was passed through "heavy glass" under the influence of an applied longitudinal magnetic field.

The theory of wave propagation in the ionosphere, supported by a series of experimental measurements, is used to demonstrate that regular amplitude variations in the structure of sweep-frequency HF oblique-ionogram one-hop rays are due to the effects of the variation of the received wave polarization with frequency. The rate of change of these variations as a function of frequency (at some instant of time) over quasi-longitudinal (QL) paths is shown to be equal to one-half the group propagation-time difference between the magnetoionic wave components at a given frequency. This relation is used to explain certain remarkable features of the rate of occurrence with frequency of the amplitude variations. Experimental measurements are described that show that the amplitude variations move with time in the frequency spectrum in a manner consistent with individual-mode CW polarization rotation with time. An experimentally based statistical description of the motion of the amplitude variations is determined as a function of both frequency and time. Computer raytracing predictions are employed to predict the variation of received skywave polarization as a function of frequency and azimuth. Polarization changes over both QL and QT (quasi-transverse) paths are considered.

When a linearly polarized CW skywave signal is received with a linearly polarized antenna, polarization rotation produces a variation of signal strength with radio frequency. The resulting amplitude vs frequency characteristic is shown to impose a bandwidth limitation on skywave transmissions where waveform preservation is important. A coherent bandwidth criterion, called polarization bandwidth, is proposed for skywave signals.

This criterion is equal to the bandwidth within which the incoming wave polarization varies 90°. It is shown that polarization bandwidth sets a more severe restriction on channel capacity than that imposed by phase distortion. Computer raytracing is employed to determine the variation of polarization bandwidth with frequency and azimuth.

A model for the ionospheric signal channel is derived whose two parameters are the rate of polarization rotation with frequency and the phase vs frequency characteristic of the path. These two quantities are shown to be readily determined from oblique-path sounding records. The general validity and usefulness of the model, and also the significance of polarization bandwidth, are demonstrated by predicting ionospheric pulse distortion over a given skywave path. It is shown that the results may be applied in choosing an optimum antenna polarization and in designing schemes for "equalizing" the dispersive parameters of the ionospheric channel.

Other applications of polarization phenomena are considered. A method for skywave communications which utilizes polarization modulation is proposed and verified experimentally. The method possesses several advantages over conventional modulation techniques. It is also proposed that by applying the relation between the magnetoionic group-time differential and the rate of change of polarization with frequency, oblique ionograms may be put into a form such that the size of valleys in, and the low-altitude values of, the electron density profile at midpath may be determined. Several techniques are proposed for utilizing the measured polarization of received skywave signals in order to register and localize ionospheric disturbances.

Chapter II

THEORY OF FARADAY ROTATION IN THE IONOSPHERE

Faraday rotation is a variation of the plane of polarization (due to the presence of a magnetic field) of time-harmonic waves propagating in a birefringent medium. At radio frequencies Faraday rotation can occur in the ionosphere. The three limiting forms of the polarization ellipse are described in this chapter. Ionospheric propagation is introduced with a discussion of the characteristic polarizations of magnetoionic wave components and the quasi-longitudinal and quasi-transverse regimes. Polarization (Faraday) rotation phenomena are then considered. A result is derived relating the magnetoionic group propagation-time differential to the frequency-rate of polarization received over a quasi-longitudinal one-hop skywave path. Computer predictions of polarization rotation are made as a function of azimuth and transmitted frequency.

A. Polarization of Radio Waves

In this section the polarization of time-harmonic, plane, propagating radio waves is defined and discussed. This subject is considered because different definitions for polarization are employed in the various fields that deal with electromagnetic phenomena. The derivation of the parameters of the polarization ellipse follows the line of Born and Wolf [2]; however, engineering conventions rather than those of optics are employed.

Polarization refers to a spatial characteristic of an electromagnetic wave at a particular point in space. In general, the wave polarization will be different at different locations, as in the case of ionospherically propagated radio waves. As used here, the term "polarization" describes the locus of the end points of the electric vector $\bar{E}$. With respect to a fixed right-handed Cartesian coordinate system (with the Z axis aligned along the wave normal), the field of a plane wave at a given location in free space may be written:

$$E_x = e_x \cos(\omega t + \phi_x)$$

$$E_y = e_y \cos(\omega t + \phi_y)$$

$$E_z = 0$$

where ω is radian frequency and ϕ is phase. Expanding the cosine term and rewriting gives:

$$\frac{E_x}{e_x} \sin \phi_y - \frac{E_y}{e_y} \sin \phi_x = \cos \omega t \sin(\phi_y - \phi_x)$$

$$\frac{E_x}{e_x} \cos \phi_y - \frac{E_y}{e_y} \cos \phi_x = \sin \omega t \sin(\phi_y - \phi_x)$$

Squaring and adding gives:

$$\left(\frac{E_x}{e_x}\right)^2 + \left(\frac{E_y}{e_y}\right)^2 - 2\frac{E_x}{e_x}\frac{E_y}{e_y} - \sin^2(\phi_y - \phi_x) = 0$$

The above equation is that of an ellipse describing the locus of the electric field vector in the plane perpendicular to the wave normal. This polarization ellipse is drawn inside a rectangle in the X-Y plane in Fig. 1. The lengths of the sides of the rectangle are $2e_1$ and $2e_2$, and Ψ is the tilt angle of the ellipse with respect to the X axis.

In order to obtain the angle Ψ (a variable which is important in describing rotating polarizations) as a function of the coordinate system orientation, it is necessary to transform the above equations to the X'-Y' axes (the axes of the ellipse). This rotation transformation may be written:

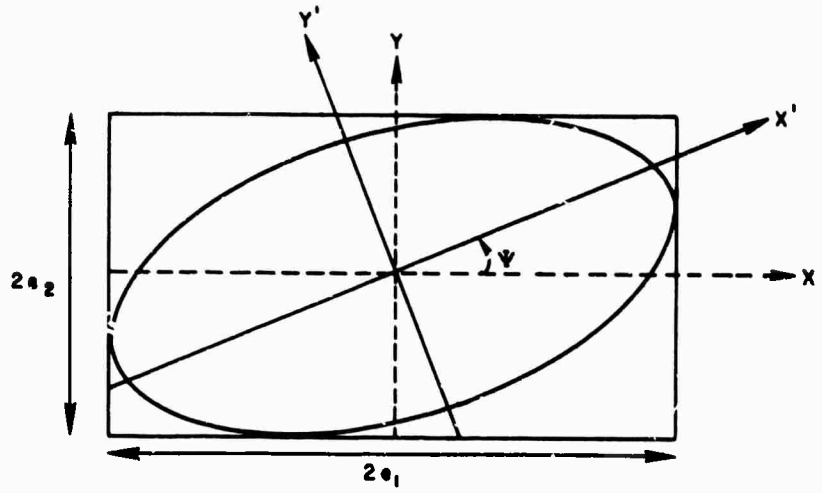

Fig. 1. THE POLARIZATION ELLIPSE.

$$E'_x = E_x \cos \Psi + E_y \sin \Psi$$

$$E'_y = -E_x \sin \Psi + E_y \cos \Psi$$

The equations of the ellipse in the primed coordinate system are:

$$E'_x = e'_x \cos (\omega t + \phi)$$

$$E'_y = \pm e'_y \sin (\omega t + \phi)$$

The $\pm$ indicates the sense of rotation of the $\bar{E}$ vector, and e'_x and e'_y are the semiaxes of the ellipse. These equations may be solved for e'_x, e'_y, and Ψ. The results are:

$$(e'_x)^2 + (e'_y)^2 = e_x^2 + e_y^2$$

$$\tan 2\Psi = (\tan 2\alpha) \cos (\phi_y - \phi_x)$$

$$\sin 2\chi = (\sin 2\alpha) \sin (\phi_y - \phi_x)$$

where $$\tan \alpha = \frac{e_y}{e_x}$$

and $$\tan \chi = \pm \frac{e'_y}{e'_x}$$

The above equations enable transformation between e'_x, e'_y, Ψ, which specify the shape of the ellipse and its orientation with respect to a fixed set of axes, and e_x, e_y, $(\phi_y - \phi_x)$, which are measurable wave parameters.

The above analysis may be extended to nonplanar waves which may occur, for example, in lossy media or for surface waves. For nonplanar waves the polarization locus is an ellipse whose shape may be related to the fields along specific axes in a manner similar to the development above. The interested reader is directed to Ref. 2.

There are three special cases of elliptical polarization. Each is characterized by certain values of $R = E_x/E_y$, the wave polarization index. Linear polarization is characterized by $R = \pm e_x/e_y$, implying $(\phi_y - \phi_x) = 0$ or some multiple of 180°. For this case the polarization ellipse reduces to a straight line; hence there will be some choice of axis orientation for which only one field component will be nonzero. Left-hand circular polarization occurs when $R = -j$, implying $|e_x| = |e_y|$ and $E_x = E_y < -90°$. For this case the field vector describes a left-hand screw as it propagates (corresponding to the direction of the fingers of the left hand when the thumb is aligned in the direction of propagation). Right-hand circular polarization is said to occur when $R = +j$.

B. The Characteristic Polarizations of the Ionosphere

The ionosphere, because of the presence of the earth's magnetic field and of electrons, is an electrically doubly refracting anisotropic medium which is slowly varying (W.K.B. approximation [3]; this approximation allows consideration of polarization phenomena using equations derived for a homogeneous medium). An arbitrary wave excited within the medium will

travel as two independent waves, each wave having a specific characteristic polarization which in general is different at each point in the medium. A characteristically polarized wave, by definition, propagates in a fixed direction with respect to the earth's magnetic field without any change in polarization. In free space a wave of arbitrary polarization propagates without any change in its polarization.

The ionospheric characteristic polarizations (at a given point in space), as determined from the Appleton-Hartree equations, fall to a good approximation within two regimes. For a typical ionospheric path at HF, the quasi-longitudinal (QL) regime occurs for angles from 0° to approximately 84° between the propagation direction and the earth's magnetic field. The two characteristic wave polarizations in this regime are nearly circularly polarized, one with a left-hand sense and the other with a right-hand sense. The quasi-transverse (QT) regime occurs for angles between 87° and 90°. The two characteristic wave polarizations in the QT regime are nearly linearly polarized, one with a major axis aligned along the earth's magnetic field and the other with a major axis aligned across the field. The angles for which propagation does not fall within one of the above regimes are a function of the relative magnitudes of the wave, plasma, and collision frequencies. Refer to Ratcliffe [4] for a discussion of the conditions under which the QL and QT regimes are valid.

When a radio wave traverses a skywave path, it may pass through both regimes. In this case, it is the exiting, or limiting, polarization that determines the wave polarization incident upon the receiving antenna. The concept of limiting polarization may also be applied when considering the manner in which the transmitted wave is split into magnetoionic components upon entry into the ionosphere.

The term "ordinary" is assigned to the QT wave whose electric vector is aligned along the earth's magnetic field. As the direction of propagation with respect to the earth's field becomes increasingly longitudinal, the ordinary mode becomes first elliptically and then circularly polarized (the QL regime) in the left-hand sense if the sign of the component of the earth's field aligned along the raypath is positive, as with downcoming waves in the northern hemisphere. The QT wave whose electric vector is aligned across the earth's magnetic field is called

"extraordinary." This term also is given to the right-hand circularly polarized QL wave whose raypath is aligned along a positive component of the earth's field.

C. Faraday Rotation

Faraday rotation in the ionosphere is due to magnetoionic splitting of the radio wave in which two components result: one ordinary and the other extraordinary. Each wave component travels through and is reflected from the ionosphere nearly independently with different phase and group velocities. The difference in phase velocities of the two modes produces the change in wave polarization. Two cases of Faraday rotation, corresponding to the QL and QT regimes, are considered. In practice, nearly all skywave paths except those disposed along the equator are quasi-longitudinal; however, it is common for east-west paths to have a small QT region located between two QL regions.

Under QL conditions, a linearly polarized wave transmitted into the ionosphere is split into two circularly polarized components of nearly equal magnitude. At any point along the path, these two modes sum to a linearly polarized wave (Fig. 2a), assuming that the two magnetoionic modes follow the same trajectory. The difference in the phase velocities between the modes causes the plane of polarization of the linearly polarized wave to rotate as the wave progresses along the path (Fig. 2b). The sense and rate of rotation are a function of the orientation of the earth's magnetic field with respect to the raypath. Specifically, the polarization tilt angle Ψ in turns (units of 360°) is given by

$$\Psi = \frac{1}{2} (P_o - P_x)$$

where P_o and P_x are the phase paths (in wavelengths) of the ordinary and extraordinary waves, respectively [5].

$$P_o = \frac{1}{\lambda} \int \mu_o \, ds \qquad P_x = \frac{1}{\lambda} \int \mu_x \, ds$$

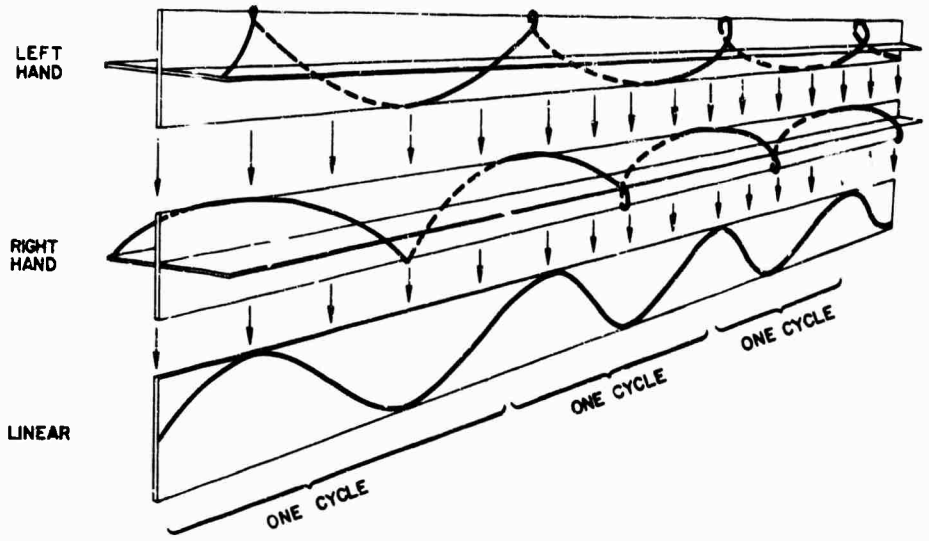

(a) Two equal-amplitude circularly polarized waves having identical phase velocities that sum to produce a linearly polarized wave of fixed polarization

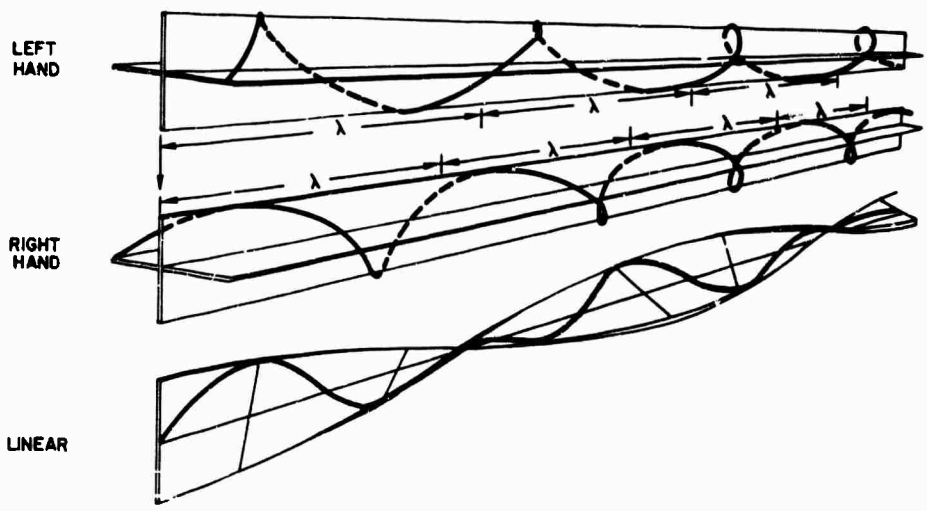

(b) Two equal-amplitude circularly polarized waves having different phase velocities that sum to produce a linearly polarized wave of rotating polarization

Fig. 2. QL FARADAY ROTATION.

where λ is the free-space wavelength, and μ_o and μ_x are the indices of refraction for longitudinal propagation. The integral is taken over the raypath. Assuming no collisions,

$$\mu_{o \atop x} = \left(1 - \frac{X}{1 \pm Y}\right)^{1/2} \qquad (1)$$

For quasi-longitudinal propagation, Y is replaced by Y_L, the longitudinal component of Y. At the receiving antenna, or at a given point along the raypath,

$$\Psi = \int_{\text{path}} \frac{\omega}{2c} (\mu_o - \mu_x)\, ds$$

where c is the speed of light in free space. Equation (1) may be written approximately as:

$$\mu_{o \atop x} = 1 - \frac{X}{2} (1 \mp Y_L)$$

when $X \ll 1$. Then

$$\mu_o - \mu_x = XY_L = \frac{\omega_N^2 \omega_H \cos\theta}{\omega^3}$$

Additional terms in the square root expansion may be employed [6]; however, higher order terms may be neglected at HF for skywave paths. Evaluating the polarization tilt angle,

$$\Psi_{QL} = \frac{e^3}{8\pi^2 m^2 \varepsilon_o c f^2} \int_{\text{path}} B_o N \cos\theta\, ds$$

where B_o is the magnitude of the earth's magnetic field, e is electronic change, f is frequency in hertz, and N is electron density. The term preceding the integral (excluding the frequency factor) has a value of 2.365×10^4 coul-m^2/kg-s in rationalized MKS units. This equation indicates that the received polarization of waves propagated over QL paths may vary with frequency and with changes in the ionospheric parameters, and that the number of polarization rotations over the path is a measure of the integrated electron content.

For QT propagation, Faraday rotation in the strict sense occurs, but there is no net accumulation of turns as under QL conditions. The phase difference between the two linearly polarized characteristic waves changes as they travel through the ionosphere. For the special case of transmitting a linearly polarized wave that excites each of two magnetoionic components equally or for a circularly polarized wave, the total wave polarization will progress cyclically from linear to elliptical to circular (of one sense) to elliptical to linear (90° rotated in polarization from the initial wave) to elliptical to circular (of the opposite sense) to elliptical to linear (identical to the transmitted wave), as shown in Fig. 3 for one linear-to-circular polarization transition. In the general case of incident elliptical or randomly aligned linear polarization, the wave polarization will vary in a complex manner, but there will always be some points in space at which the polarization is linear.

D. Computer Prediction of HF Oblique-Path Polarization Rotation with Frequency and Azimuth

The purpose of this section is to predict the manner in which oblique-path polarization rotation varies as a function of raypath azimuth and transmitted frequency. It was shown in Section C that, for an oblique skywave path under QL conditions, the incoming wave polarization incident upon the receiver is directly proportional to the phase path difference between the extraordinary and the ordinary rays. Thus, any physical phenomenon that varies the phase paths would change the received polarization with time; examples are slow internal ionospheric motions and changes in satellite location (for satellite-earth paths).

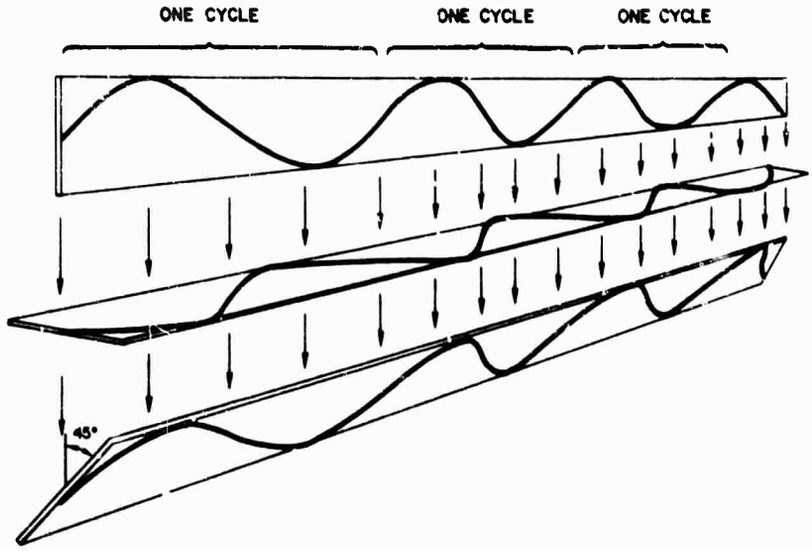

(a) Phase difference of 0^{o} producing linear polarization

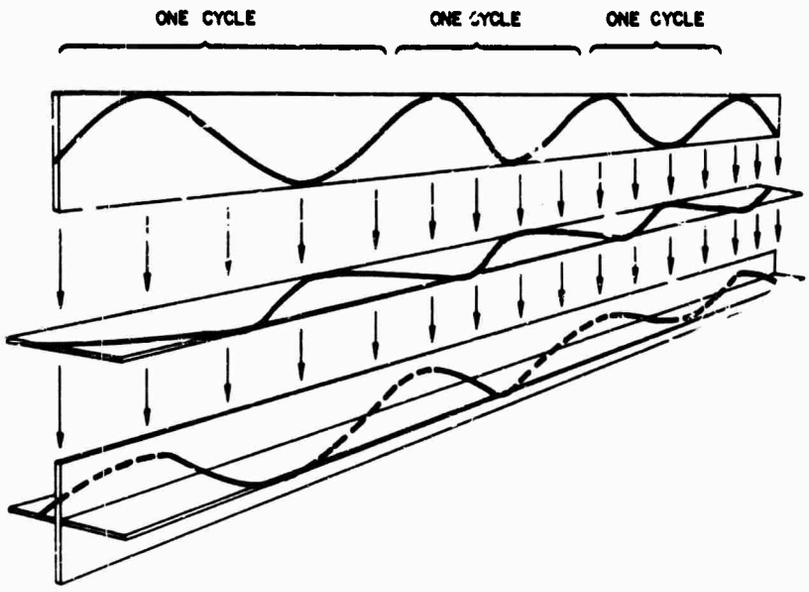

(b) Phase difference of 45^{o} producing elliptical polarization

Fig. 3. QT FARADAY ROTATION.

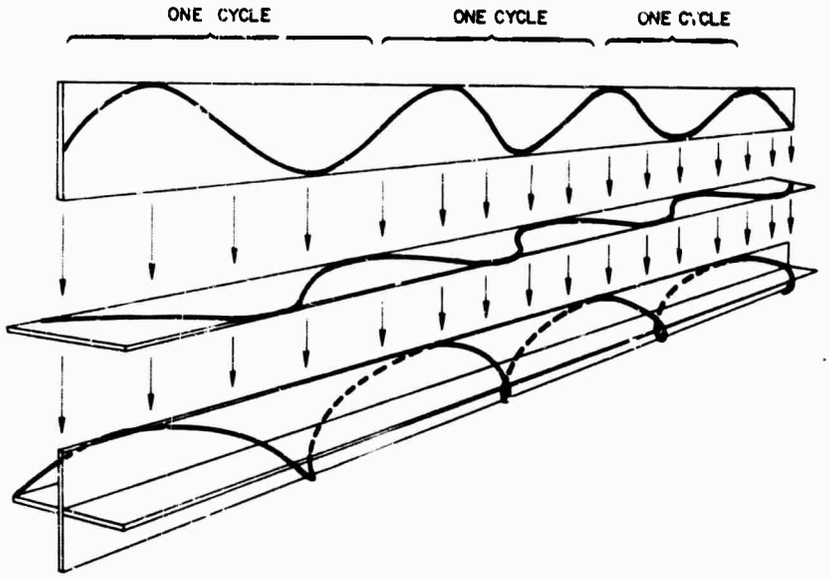

(c) Phase difference of 90° producing circular polarization

Fig. 3. CONTINUED.

For single mode paths (e.g., one-hop lower ray), polarization changes with time produce alternate signal strength maxima and nulls as a function of the angle between the received polarization and the receiving antenna. In the polarization-rotation-with-frequency case the relative phase between the extraordinary and the ordinary components varies with frequency, partially because of changes in raypath trajectory, so as to produce a linearly polarized wave whose plane of polarization rotates with frequency. In a linearly polarized receiving antenna such a wave produces signal amplitude variations with frequency. This amplitude vs frequency characteristic, which may be characterized by the rate of polarization rotation with frequency (abbreviated to "frequency rate"), can be detrimental to the transmission of broadband and/or short-pulse skywave signals. This subject will be discussed in detail in Chapter IV.

Calculations were performed with a digital computer raytracing program developed by Croft [7] using the quasi-longitudinal approximation. The program input consists of ionospheric electron density vs height,

takeoff elevation angle and azimuth of transmitted rays, transmitted frequency, and transmitter latitude. The output consists of the total polarization rotation for the ground range at which each ray hits the earth. (Elevation angles for each frequency are chosen so that the transmitted rays land in the neighborhood of a fixed ground range; the polarization rotation can then be determined by interpolation.) By performing the calculations for many frequencies, polarization rotation as a function of frequency for one-hop paths is found. In addition to the polarization rotation information, the computer also calculates the no-field group and phase time delays incurred by each ray.

The number of polarization rotations executed by a one-hop signal as it travels from the transmitter into the ionosphere and reflects back to a receiver on the ground was determined as a function of frequency for rays transmitted at an azimuth of 45° east of magnetic north, and as a function of azimuth for 10.5 and 17.5 MHz. All calculations were made assuming a transmitter location at a latitude of 38° and a receiver location at 2000 km ground range from the transmitter. The concentric, single-layer Chapman ionosphere that was employed is shown in Fig. 4 together with the corresponding 2000 km, computer-generated oblique ionogram [8]. The vertical critical frequency was 9 MHz, giving a path maximum usable frequency of about 21.5 MHz. A dipole approximation to the earth's magnetic field aligned with geographic coordinates was employed.

Polarization rotation vs frequency for the 45° azimuth case is presented in Fig. 5 with the corresponding polarization rotation rate. Polarization rotation rates as a function of azimuth for 10.5 and 17.5 MHz are given in Fig. 6. The results are symmetric about the geomagnetic meridian. Figure 7 shows the corresponding phase time delay $(1/c \int \mu \, ds)$ vs frequency for the no-field case. The phase time delay varies almost linearly at 5.7 μs/MHz for 10.5 MHz and at 7 μs/MHz for 17.5 MHz. Polarization rotation is not defined near the MOF (maximum observable frequency) of the one-hop mode because only the extraordinary mode is present.

The results indicate that the frequency rate of polarization increases with increasing frequency and with increased alignment of the longitudinal component of the earth's magnetic field along the raypath. This effect is expected since higher frequencies follow longer paths

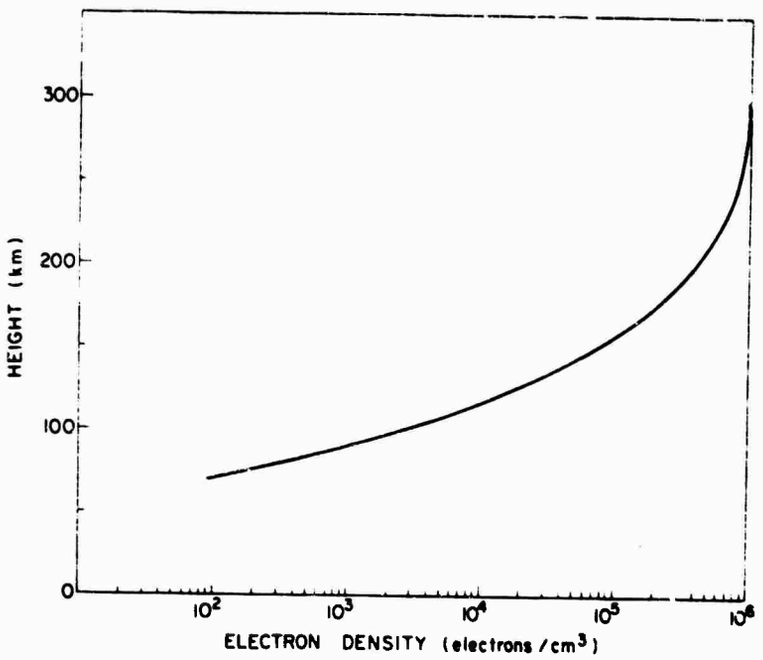

(a) Electron density profile

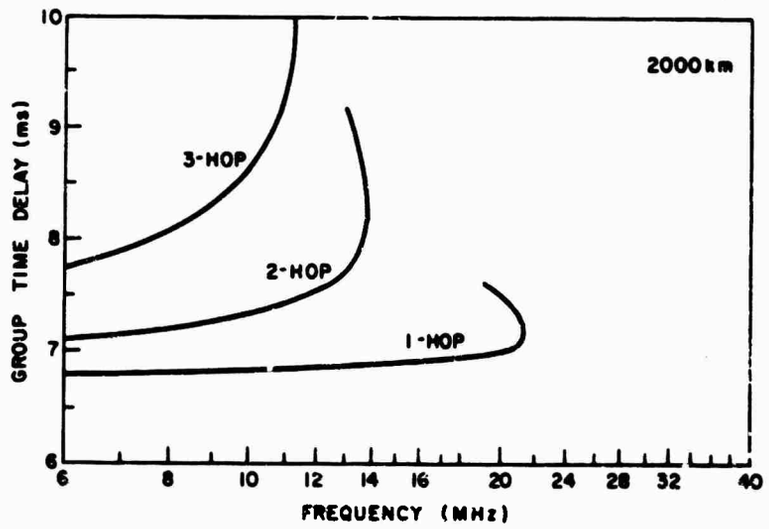

(b) Corresponding 2000-km, computer-generated oblique ion gram

Fig. 4. IONOSPHERIC MODEL.

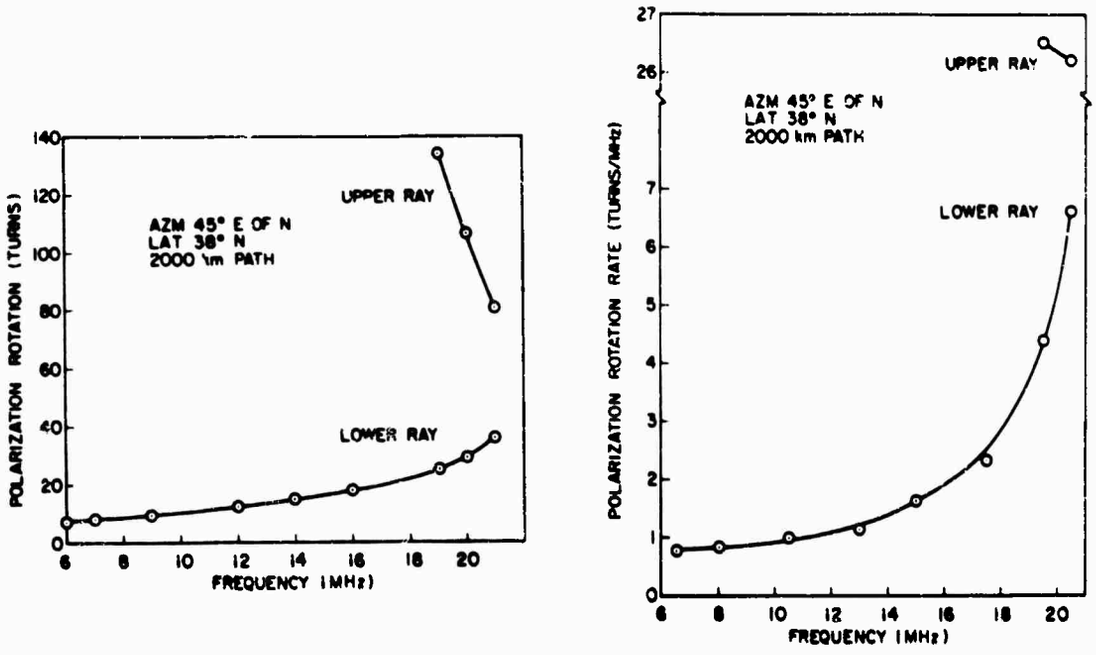

(a) Polarization rotation (b) Polarization rotation rate

Fig. 5. POLARIZATION ROTATION AND POLARIZATION ROTATION RATE AS A FUNCTION OF FREQUENCY.

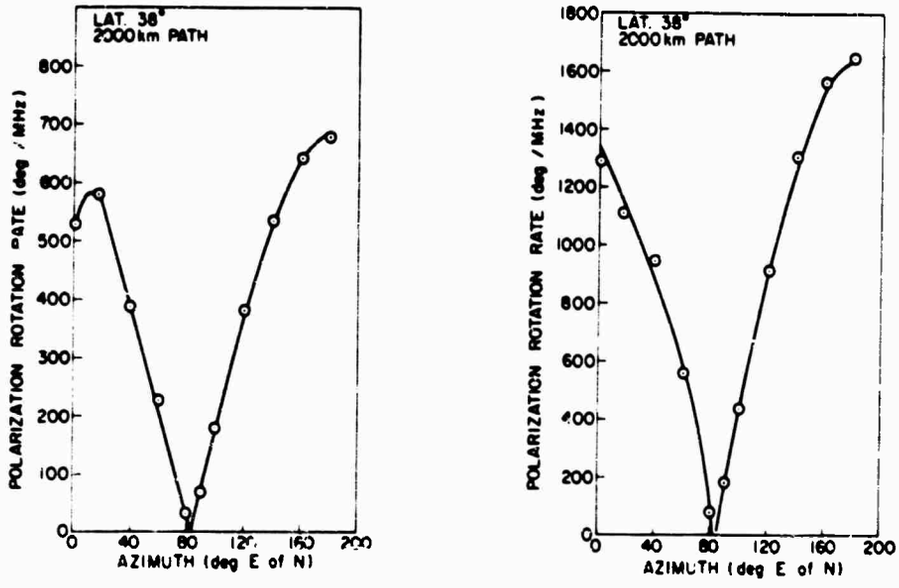

(a) 10.5 MHz (b) 17.5 MHz

Fig. 6. POLARIZATION ROTATION RATE AS A FUNCTION OF AZIMUTH. Azimuth indicates receiver location relative to transmitter.

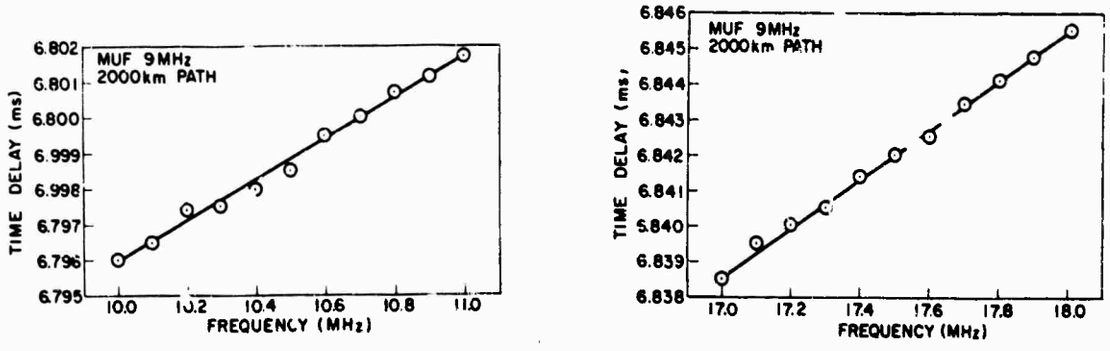

(a) 10.5 MHz (b) 17.5 MHz

Fig. 7. PHASE TIME DELAY AS A FUNCTION OF FREQUENCY.

between transmitter and receiver. The results also predict the occurrence of alternate received signal strength maxima and nulls whose rate of occurrence corresponds to that of polarization rotation. It follows from the above discussion that polarization is not defined for a pulse or any other signal whose transform possesses many frequency components, for each component may possess a different polarization.

E. The Relation between Group Time Delay and Polarization Rotation

A new relation between the frequency rate of polarization rotation and the group propagation-time difference between magnetoionic components will now be derived. The number of cycles of polarization rotation that a wave undergoes while traveling over a QL ionospheric path is equal to one-half the difference between the phase paths (in wavelengths) of the ordinary and extraordinary components. It follows that the frequency rate of polarization rotation at the receiver is

$$\frac{\partial \gamma}{\partial f} = \frac{1}{2}\left(\frac{\partial P_o}{\partial f} - \frac{\partial P_x}{\partial f}\right) \tag{2}$$

Bennett [9] recently demonstrated that the well-known relation between group time delay and phase,

$$T_g = \frac{\partial P}{\partial f} \tag{3}$$

may be applied in a slowly varying medium (with no collisions) even when the ray direction and the wave normal do not coincide. Combining Eqs. (2) and (3),

$$\frac{\partial \Psi}{\partial f} = \frac{1}{2} (T_{go} - T_{gx}) \tag{4}$$

Thus a polarization rotation rate of 1 turn/MHz corresponds to a 2 μs group time difference. The right-hand side of Eq. (4) can be either positive or negative.

The frequency rate of polarization rotation may be determined, if linearly polarized antennas and narrowband sounding signals are employed, by observing the variations in received signal strength as a function of frequency. However, this technique provides only the absolute value of the left-hand side of Eq. (4). The ambiguity may be resolved, if an oblique ionogram is available, by following the sign of the right-hand side of the equation from the junction frequency or upper ray of the mode being considered. The extraordinary MOF will always exceed that of the ordinary. The ambiguity may also be eliminated if the phase difference between characteristic modes is measured directly.

In applying the above result to oblique-path sounding it is helpful to view both the magnetoionic group propagation-time difference and the frequency rate of received polarization as characteristics of the raypath. It is assumed that the radio frequency interval between soundings, as well as the bandwidth of the probing signal, is appreciably smaller than the bandwidth required for one turn of incoming polarization. The terminal equipment employed determines to a large extent whether one experimentally observes signal amplitude variations with frequency or the two magnetoionic components on an ionogram, or alternatively, whether a single distorted pulse or two less-distorted pulses is received.

Consider a single very short pulse transmitted over a path in which the ordinary and extraordinary group time difference is larger than the pulse duration. Assuming negligible phase distortion (which may lengthen the pulse), an ideal receiver (one with perfect time delay resolution) would receive two undistorted pulses. If the receiver resolution was not

perfect, each transmitted pulse would produce a pulse with "tails" due to ringing within the receivers. If the tails of the two pulses overlap, the resulting amplitude is a function of the relative phase between each of the pulses' frequency components.

The above results are not valid for all ionospheric paths. Specifically, the relation cannot be applied to paths possessing a QT region located between two QL regions, because the sign of the longitudinal component of the earth's magnetic field changes as the QT region is crossed. Under these conditions the polarization angle which has been "winding up" on one of the QL paths, for example, winds in the opposite direction on the other path. This effect occurs because of an interchange of the sense of circular polarization from one magnetoionic mode to the other, since $R = -j|Y_L|/Y_L$ for QL paths. The index of refraction μ is not affected by the sign change; thus, the group time difference between modes continues to increase on the second part of the path. The problem of determining satellite-to-earth integrated electron content in the presence of QT regions by CW polarization rotation measurements is discussed by Dulk [10].

BLANK PAGE

Chapter III

POLARIZATION MEASUREMENTS

When an HF skywave signal is received on a linearly polarized antenna, polarization rotation in the ionosphere may produce a variation of received signal strength with both time and radio frequency, as shown theoretically in the previous chapter. Oblique-path HF measurements are now described which were designed to investigate the phenomenon of polarization rotation with frequency and to confirm theoretical predictions. The experiments utilized a high resolution FM-CW sounding system operated over the 1900 km east-west temperate zone path from Lubbock, Texas to Stanford, California, as shown in Fig. 8. Cross-polarized log-periodic receiving antennas were employed to provide vertically, horizontally, and circularly polarized reception simultaneously. A horizontal rhombic antenna was also employed for some tests.

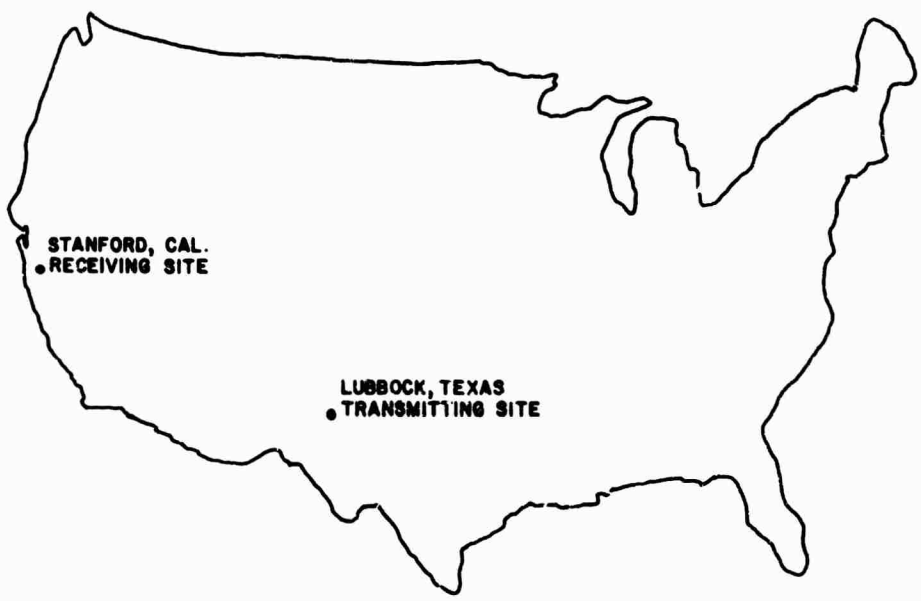

Fig. 8. TRANSMITTING AND RECEIVING SITE LOCATIONS.

Measurements were performed to determine the frequency rate of polarization rotation as a function of frequency, and to obtain a description

of polarization-induced amplitude nulls appearing on group time delay vs transmitted frequency records (oblique ionograms). An experimental procedure, fundamental to the design of adaptive communication systems, was developed for obtaining a correlation description of the amplitude and phase of the ionospheric channel. Certain anomalous variations in the frequency rate of polarization rotation as a function of frequency, which were not predicted by the calculations of Section II-D, are explained by applying the theoretical relation between magnetoionic group time differential and polarization rate derived in Section II-E.

A. Experimental Arrangements

1. FM-CW Sounding System

Sweep-frequency CW sounding equipment, developed by Fenwick and Barry [11], was employed. The receiving equipment is shown in Fig. 9.

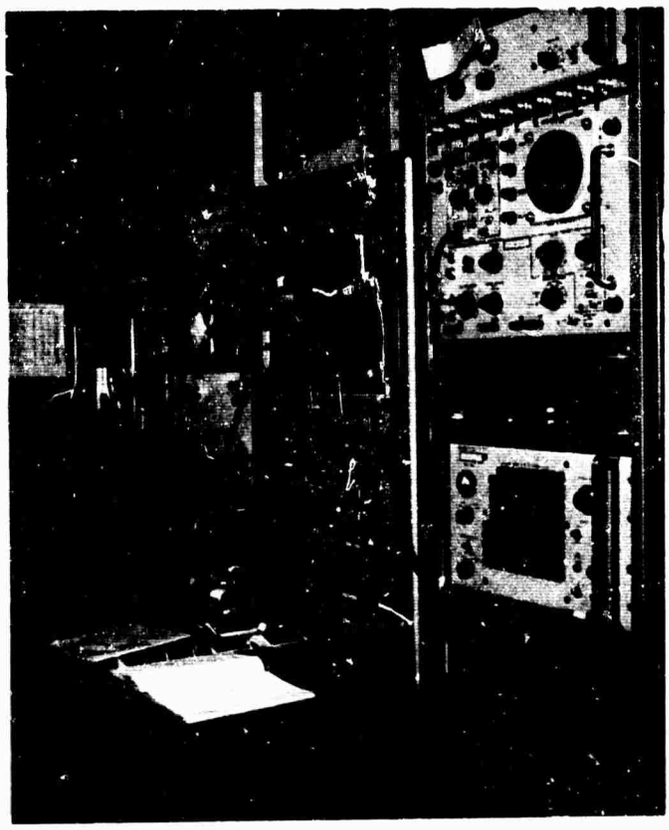

Fig. 9. RECEIVING EQUIPMENT.

Two similarly modified frequency synthesizers were employed, one for use as a transmitter exciter and the other to generate the receiver first-mixer injection signal. A close approximation to a CW signal having a linearly increasing frequency is generated by rapidly and phase coherently switching the synthesizer frequencies as shown in Fig. 10. Operation of

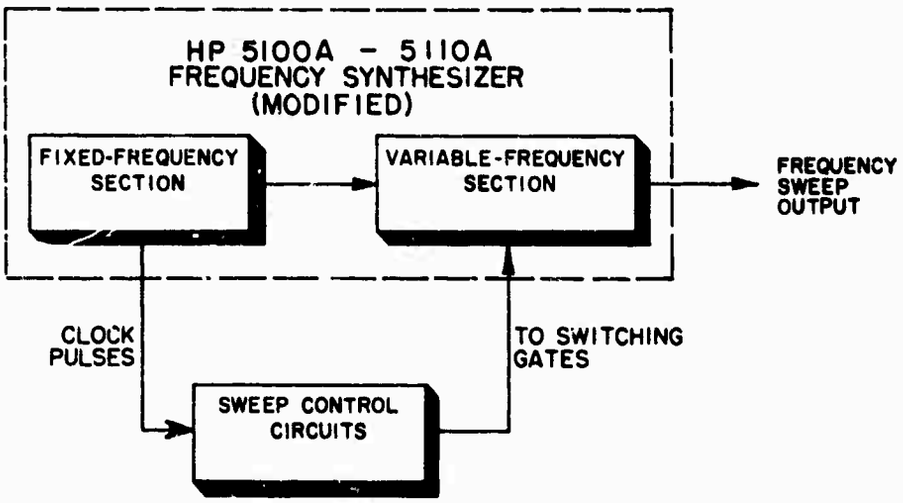

Fig. 10. BLOCK DIAGRAM OF FREQUENCY-SWEEP SYSTEM.

the sounding system proceeds as follows: The transmitted signals arrive at the receiver with each frequency component of the sweep-frequency signal phase shifted and attenuated according to the characteristics of the ionospheric channel transfer function. The signal is mixed with a replica of the transmitted waveform which has been translated up in frequency (by 18 MHz) to produce an IF signal. The IF signal is received by a communications receiver employing product detection to produce an audio signal which is recorded on magnetic tape. Since a linear frequency sweep is employed, calibration marks placed on the tape to indicate the beginning of a sweep allow the transmitted frequency to be determined.

The phase of the audio signal during a frequency sweep corresponds to the phase vs frequency characteristic of the ionosphere. Hence, when the frequency components of the signal are displayed with a spectrum analyzer, the components that appear are a measure of the relative group propagation-time delay through the channel. This relation assumes that

the ionospheric doppler shifts due to motions within the ionosphere are negligible compared with frequency shifts due to group propagation-time delay changes. For a 1 MHz/s FM-CW sweep (the sweep rate for the experiments here described) ionospheric doppler shifts on the order of 1 Hz produce a 1 μs group time shift, much less than the group time accuracy required. A Mod. 480-10 Spectran spectrum analyzer was employed.

The amplitude of the received FM-CW signal corresponds to the amplitude transfer function of the ionosphere. Hence a display of frequency vs time vs amplitude (in the 2 dimension) corresponds to the group time vs frequency description of the ionospheric channel called an oblique ionogram (see Fig. 11). Unless extremely accurate frequency standards are employed to synchronize timing pulses at the transmitter and receiver, the oblique ionogram displays only relative group time over the path. For the purposes of studying ionospheric polarization effects, this level of accuracy is sufficient.

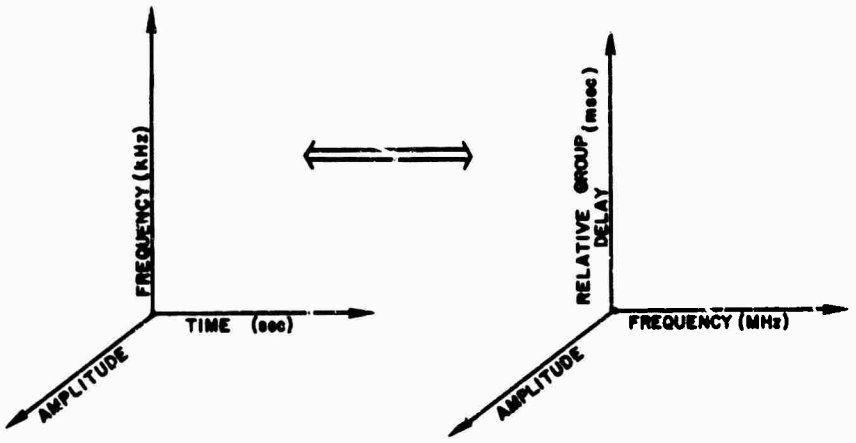

Fig. 11. THE EQUIVALENT REPRESENTATIONS EMPLOYED TO RELATE FM-CW SOUNDER OUTPUT TO OBLIQUE IONOGRAMS.

2. Antennas

Two types of receiving antennas were employed, one of which was designed and built for the polarization experiments. This latter antenna consists of two Hy-Gain LP-13-30 log-periodic arrays, shown in Fig. 12,

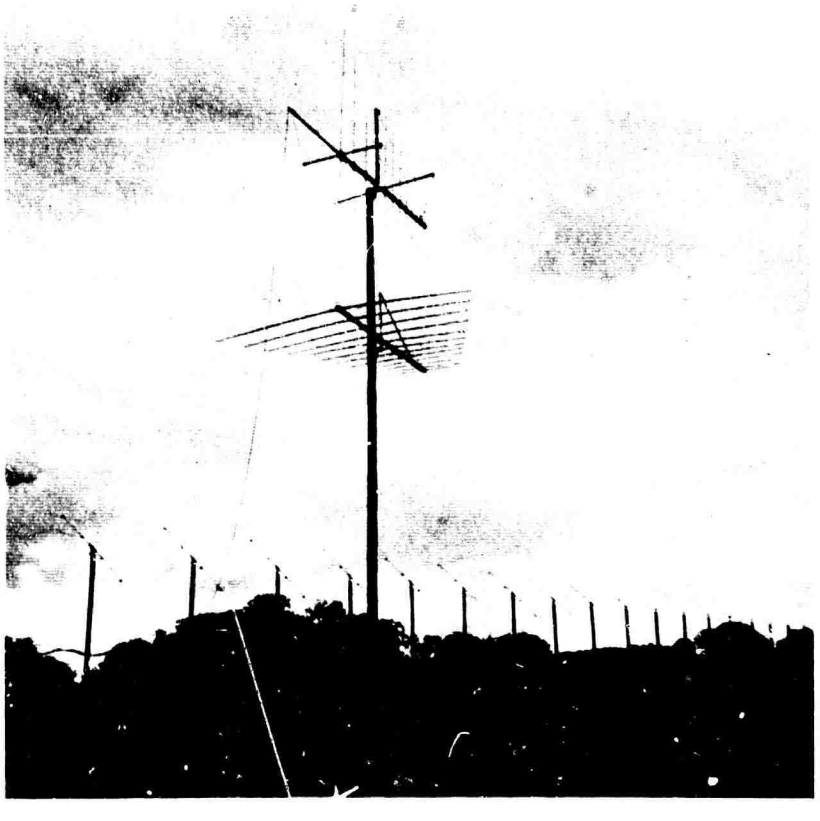

Fig. 12. CROSS-POLARIZED RECEIVING ANTENNAS.

both pointed toward the transmitting site. The Yagi antennas shown on the left of Fig. 12 are used in the forward field of view of the log-periodic antennas. One of the receiving antennas is mounted vertically at 76 ft height; the other is mounted horizontally at 54 ft. These heights were chosen so that the mainlobe vertical patterns would nearly coincide. The ground slopes at about 5° upward in front of the antennas. Cross-coupling between the antennas was determined experimentally to be better than 40 dB across most of the HF band. VSWR vs frequency curves for the antennas were determined and found to be nearly identical. Signals from these two antennas reach the receiving trailer through approximately 1200 ft of equal-length RG-8 cable, introducing about 20 dB loss. The signals from the two antennas were combined to provide a circularly polarized antenna capability. For the case in which the vertical antenna is obtained by rotating the horizontal antenna longitudinally 90° in a counterclockwise direction from the rear, a 90° phase-shift network inserted in the cable to the horizontally

polarized antenna creates an antenna pair whose sum and difference signals correspond to that which would have been received with a left- and right-hand circularly polarized antenna, respectively (see Fig. 3c). For the FM-CW experiments, a 90° phase-shift network was inserted at the receiver IF frequency. An Adams-Russell HH-50 hybrid junction sum-difference network was employed. Signal power-splitting and mixing operations were performed with a Trak Model 108 antenna multicoupler, Adams-Russell TN-50 Iso-T's, and Hewlett-Packard Model 10514-A mixers.

The second type of receiving antenna, employed for two of the experiments, is a horizontal rhombic antenna with a leg length of 183 ft and a total length of 361 ft.

For most transmissions a horizontally polarized Granger Associates Model 747L wire log-periodic antenna mounted between two 140-ft steel towers was employed. A cross-polarized log-periodic pair similar to that described above was used for experiments discussed in Chapter V.

B. Experiments To Confirm the Existence of Polarization Rotation with Frequency

The existence of polarization rotation with frequency was confirmed by performing a series of four experiments in which amplitude vs frequency records of individual modes of propagation were obtained. The frequency of the appropriate audio output signal of a high-frequency FM-CW oblique-path sounder corresponds to the corresponding path group time delay. These data allow individual modes (e.g., one-hop lower rays) to be selected by simple bandpass filtering. The selected signal can be subsequently displayed on a chart recorder to provide a record of signal amplitude vs frequency along a given ray. A typical winter-noon oblique ionogram is shown in Fig. 13 with the chart-recorded amplitude vs frequency behavior of its one-hop lower ray. The ionogram was made by sweeping the FM-CW sounder over the 4 to 30 MHz band. Only traces corresponding to F-layer reflections appear because the transmitting antenna pattern does not favor low-angle (or E-layer) modes, and because the receiving antenna has a similar characteristic due to shielding by a nearby hill. An explanation for the sharply defined amplitude nulls appearing

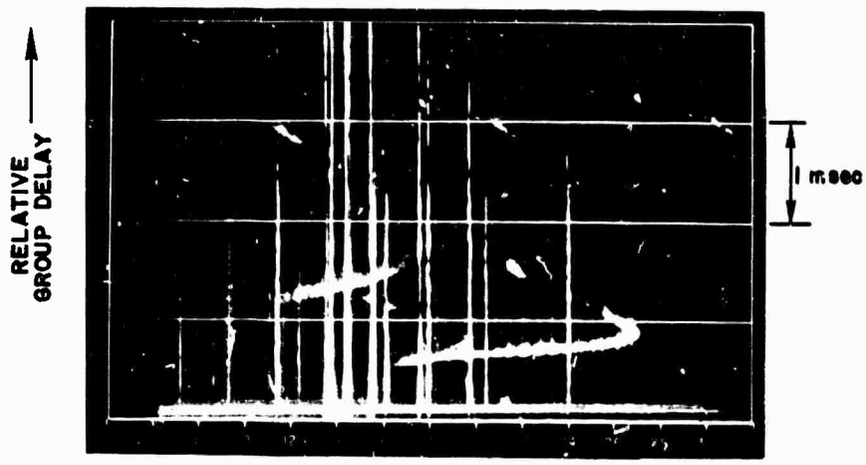

(a) Oblique ionogram

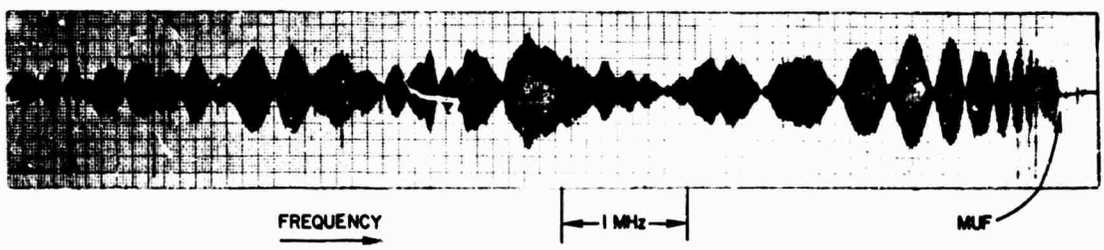

(b) Amplitude vs frequency behavior of the one-hop lower ray

Fig. 13. EXAMPLE OF DATA-REDUCTION TECHNIQUE.

on the records is provided by the first experiment. All signals were transmitted with a power of approximately 60 W.

The first experiment, performed 1 March 1967, employed one receiver (a Hallicrafters MHR-2S-1) whose input was rapidly switched from the horizontally to the vertically polarized antenna. A block diagram of the experiment is shown in Fig. 14. Ionospheric conditions during the experiment correspond to those shown in Fig. 13a. The coaxial relay was switched at a 5 Hz rate, thereby alternately sampling a 100 kHz bandwidth every 0.1 sec from each antenna. A display of the amplitude vs frequency behavior of the one-hop lower ray using this technique is shown in Fig. 15.

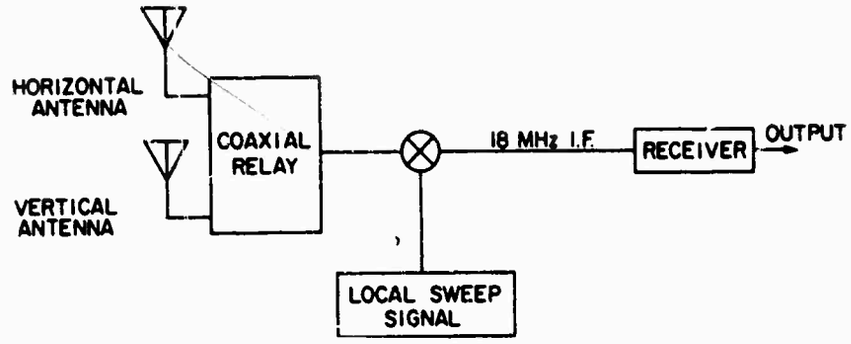

Fig. 14. BLOCK DIAGRAM OF ANTENNA-SWITCHING EXPERIMENT.

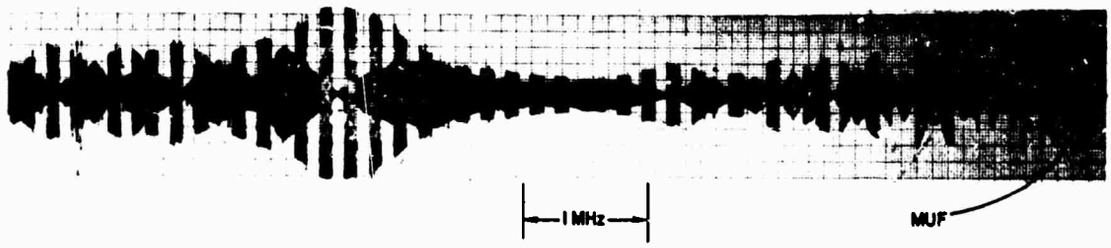

Fig. 15. AMPLITUDE VS FREQUENCY BEHAVIOR OF THE ONE-HOP LOWER RAY DURING ANTENNA-SWITCHING EXPERIMENT.

This record demonstrates that when a signal null appears at a given frequency on one of the linearly polarized antennas, a signal maximum appears at the same frequency on the orthogonal antenna. This suggests that (1) the incoming polarization is linearly polarized, and (2) it is rotating with frequency. The latter effect is clearly demonstrated, however, only in the slow polarization-rotation region at the left-hand side of the record shown in Fig. 15.

Accordingly, on 3 March 1967 a more complex experiment was performed which involved simultaneous reception of signals on the two orthogonal linearly polarized antennas, as shown in Fig. 16. Collins 75S-3 receivers were employed. The amplitude vs frequency characteristics of one-hop lower rays received simultaneously in this manner are presented in Fig. 17. Part of the ionogram made from signals received on the horizontally polarized antenna is also shown. One can compare the amplitude vs frequency record of the horizontally polarized chart-recorded signal "blob

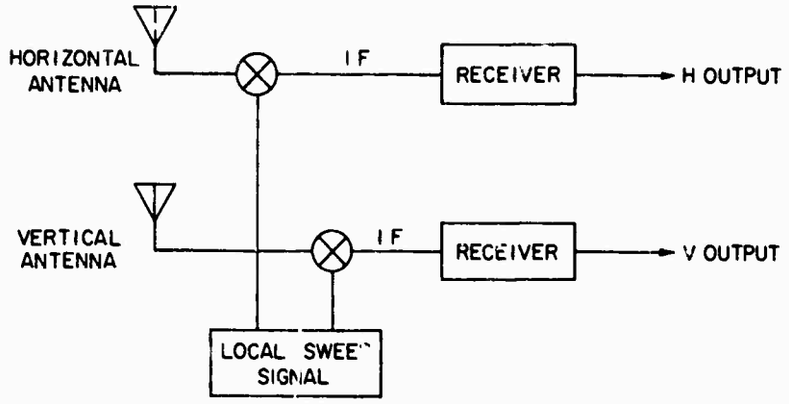

Fig. 16. BLOCK DIAGRAM OF THE TWO-RECEIVER EXPERIMENT.

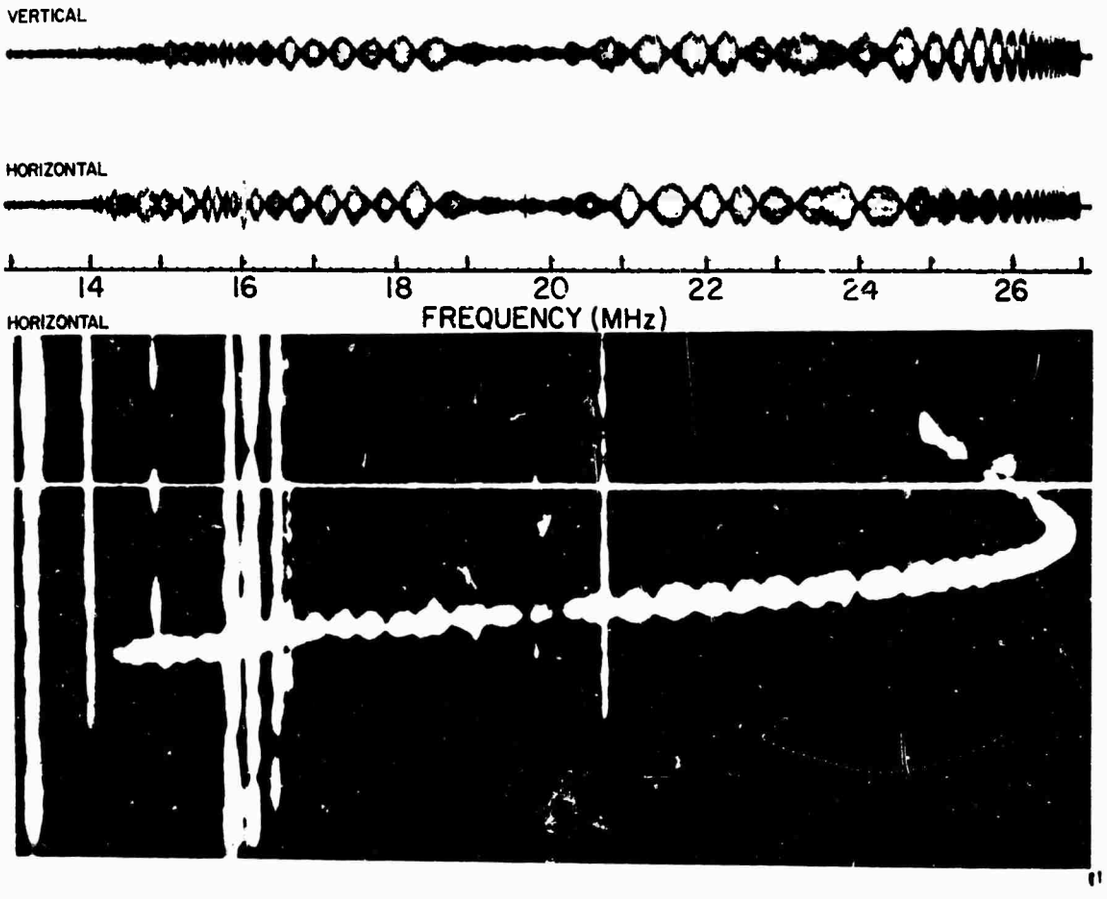

Fig. 17. RESULTS OF THE TWO-RECEIVER EXPERIMENT.

for blob" with the oblique-ionogram record. The data confirm the results of the first experiment for all frequencies of the one-hop lower ray, even for that part of the ray when the null rate is most rapid (near the MUF). The 90° phase shift observed in the outputs of the two antennas is expected from the theoretical rotating linear polarization model.

The results shown in Fig. 17 suggest that the frequency rate of polarization rotation first decreases and then increases with increasing frequency along the one-hop lower ray. A graph of polarization rotation rate vs frequency is shown in Fig. 18. Polarization rotation rate is

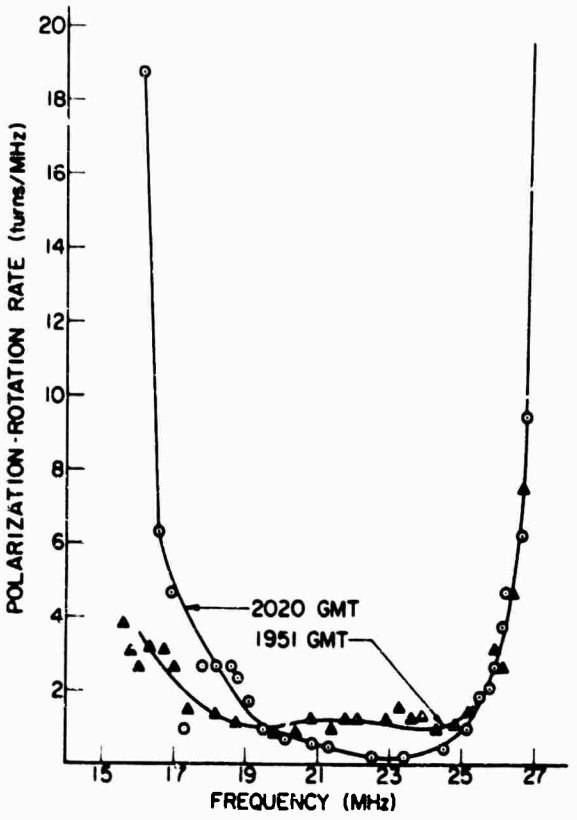

Fig. 18. EXPERIMENTALLY DETERMINED POLARIZATION ROTATION RATE VS FREQUENCY.

obtained by measuring the bandwidth subtended by successive amplitude nulls as a function of frequency. The incoming polarization rotates 180° between these nulls. Similar variations of polarization rate were observed on nearly all soundings made over this path since the experimental

equipment was first installed in December 1966. This effect, which is not predicted by the calculations of Section II-D, is discussed in Section C below.

In order to demonstrate more clearly the effects of polarization rotation as a function of frequency, and also to test one of a number of methods for eliminating the amplitude vs frequency variations produced by polarization rotation, signals were received simultaneously using horizontally and vertically polarized antennas and both senses of circularly polarized antennas on 14 April 1967 at local noon. A block diagram for the experiment is shown in Fig. 19. (The square boxes in the figure are

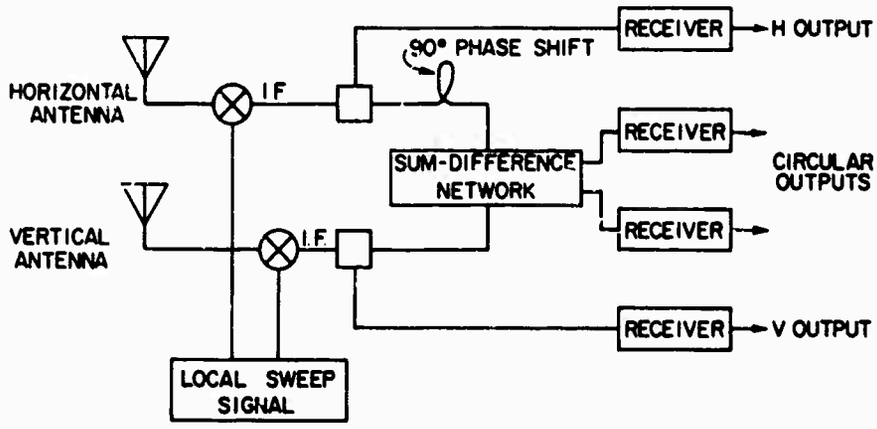

Fig. 19. BLOCK DIAGRAM OF THE CIRCULARLY POLARIZED ANTENNA EXPERIMENT.

power splitters.) Theoretically, variations in the incoming polarization angle of a linearly polarized wave should not affect signals received on a circularly polarized antenna. The results of this experiment is best demonstrated by comparing four simultaneously recorded ionograms, shown in Fig. 20. The nulls appearing on the records of the linearly polarized antennas do not appear on those made with the circularly polarized pair. The horizontal trace near the bottom of Fig. 20c is due to 60 Hz hum.

Repetitive FM-CW sounder transmissions over the 18 to 19.5 MHz band were transmitted over the Lubbock-Stanford path at 1840 GMT on 17 December 1966. The signals were received on the rhombic antenna in order to provide polarization data simultaneously over a portion of the upper and

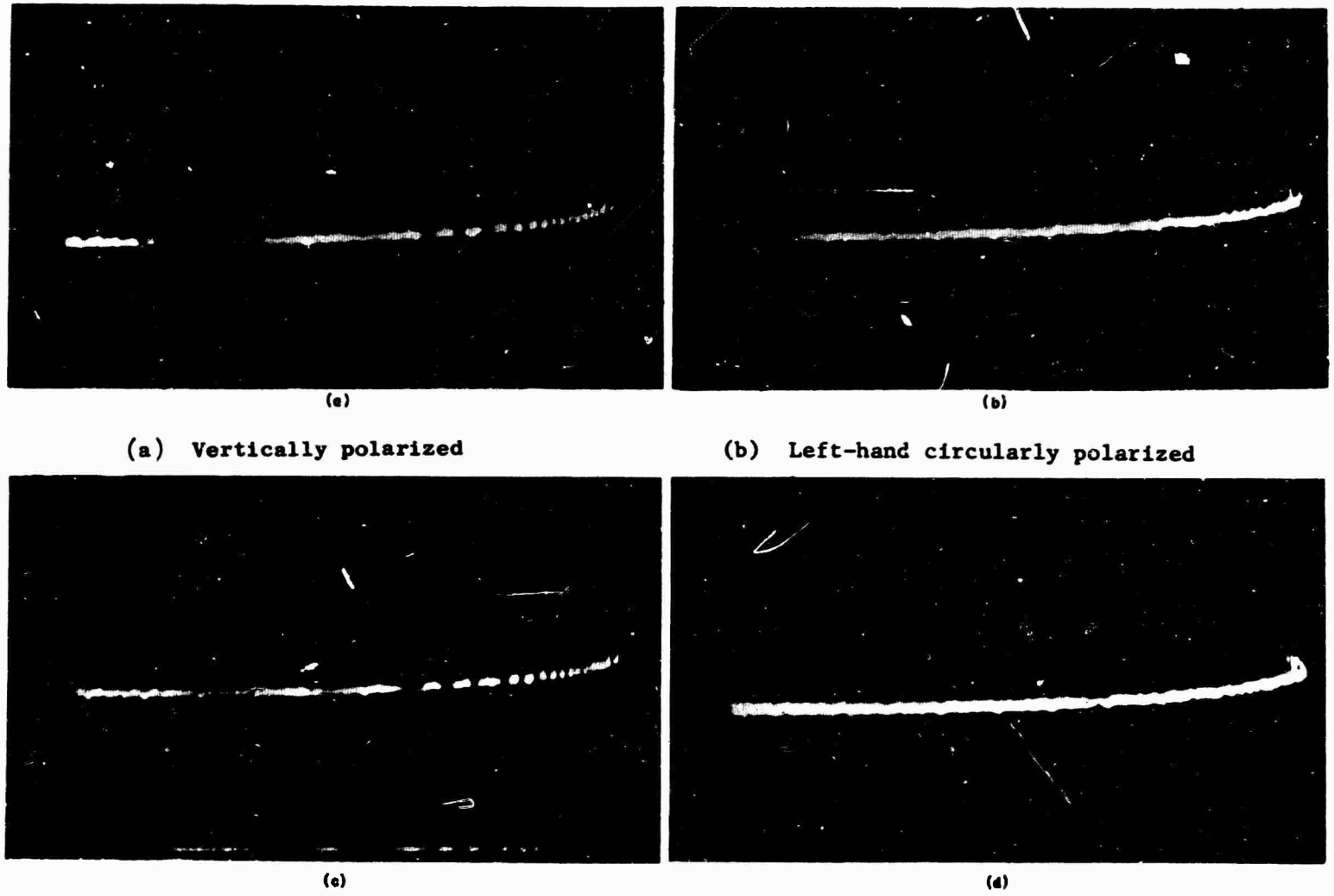

(a) Vertically polarized

(b) Left-hand circularly polarized

(c) Horizontally polarized

(d) Right-hand circularly polarized

Fig. 20. SIMULTANEOUS IONOGRAMS FROM LINEARLY AND CIRCULARLY POLARIZED ANTENNAS.

lower one-hop rays. An ionogram made prior to the test is shown in Fig. 21. A half-second dead time was inserted between each 1.5 sec sweep to

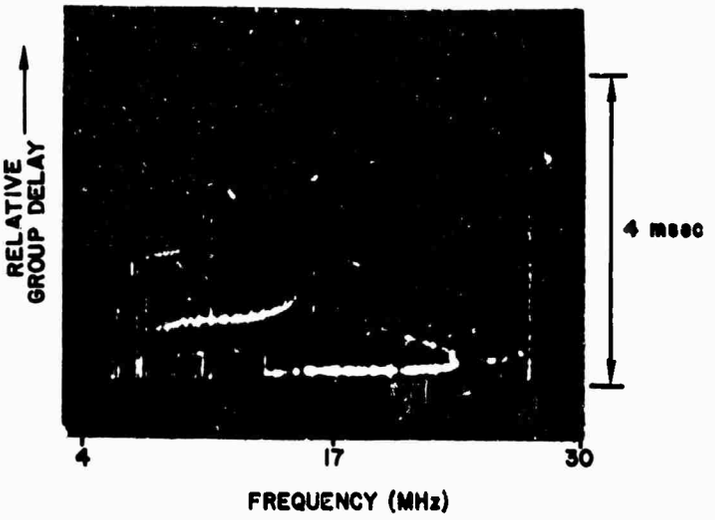

Fig. 21. IONOGRAM MADE PRIOR TO UPPER- AND LOWER-RAY POLARIZATION MEASUREMENTS.

provide frequency and time calibration. Data were taken in this manner for 5 min. A typical group delay vs frequency record of the repetitive sweeps is shown in Fig. 22 together with the amplitude vs frequency records of the upper and lower rays. The modes were separated with two bandpass filters. The experiment showed that the upper ray of one-hop modes possesses amplitude fluctuations due to polarization rotation with frequency that are far higher than those of the lower ray. This result, predicted by the computer calculations of Chapter II, is interpreted in Section C.

C. Comparison with Theoretical Predictions

The theoretical predictions of the frequency-rate of polarization rotation presented in Chapter II do not account for the anomalous variation of polarization rotation rate along the lower ray of the one-hop mode. This effect may be understood by applying the results of Chapter II-E. It was found experimentally that for the one-hop lower ray, the polarization rotation rate invariably first decreased with increasing

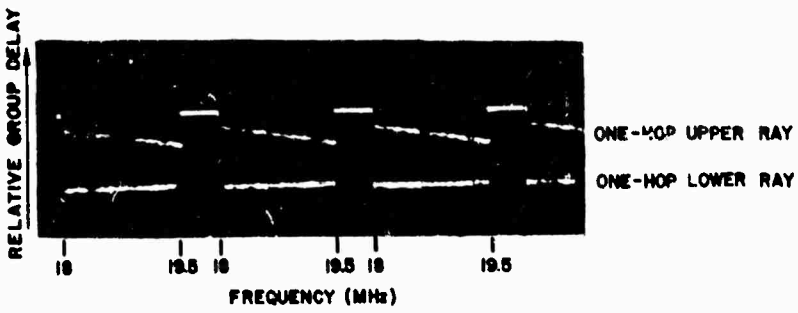

(a) Ionogram representation of signals

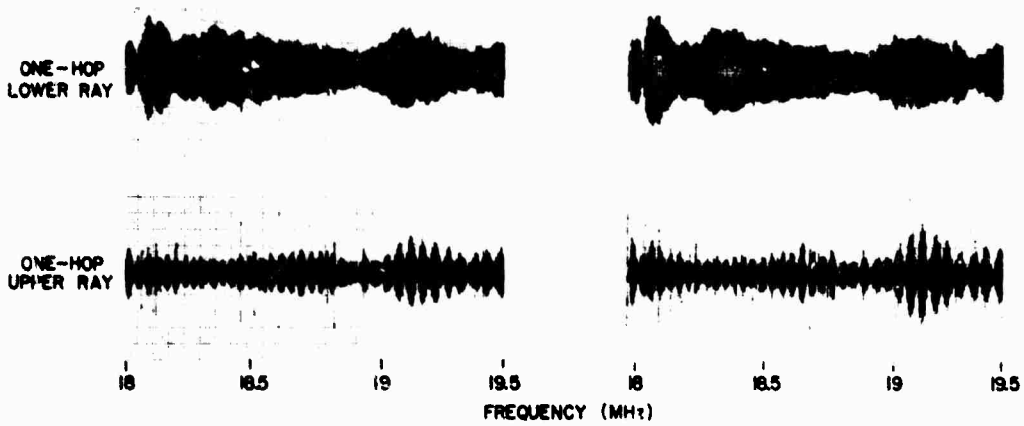

(b) Chart recorded signals

Fig. 22. AMPLITUDE VS FREQUENCY BEHAVIOR OF THE UPPER AND LOWER ONE-HOP RAYS.

frequency (polarization blobs getting longer), and then increased with increasing frequency until the MOF was reached. A possible explanation for this phenomenon is that, as the frequency increases, the two magnetoionic components become closer together in relative time delay, cross, and then separate again, as shown in Fig. 23. This effect is believed due to the presence of lower ionospheric layers not included in the theoretical model.

Experimental confirmation of the group time and polarization equivalence was obtained by processing the group time vs frequency record of

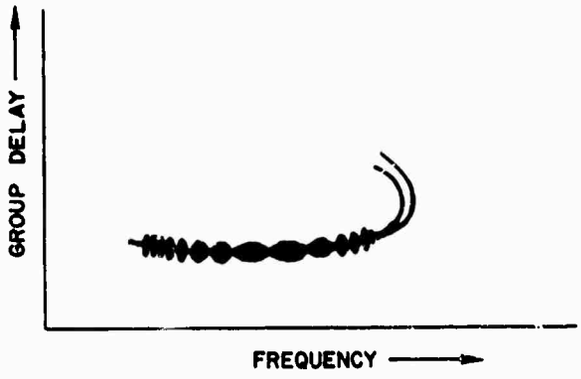

(a) Low-resolution record

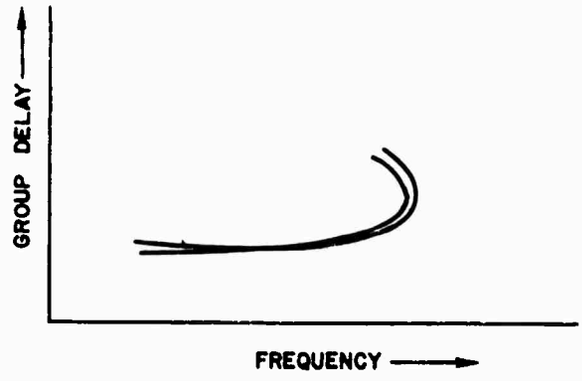

(b) High-resolution record

Fig. 23. EQUIVALENT REPRESENTATIONS BY POLARIZATION NULLS AND DIFFERENTIAL GROUP DELAY.

Fig. 22 to a higher resolution. Higher resolution was obtained by playing the audio-frequency data tape into the spectrum analyzer at four times the real-time speed. This has the effect of narrowing the bandwidth analyzed by each filter. The results, shown in Fig. 24, indicate that the upper-ray blobs of Fig. 22 are actually two magnetoionic rays. The decreasing rate of polarization nulls at higher frequencies observed in Fig. 22b is due to a decreasing group time spacing of the ordinary and extraordinary rays. The fine, evenly spaced vertical lines in Fig. 24 are due to individual oscilloscope traces. The group time delay spacing

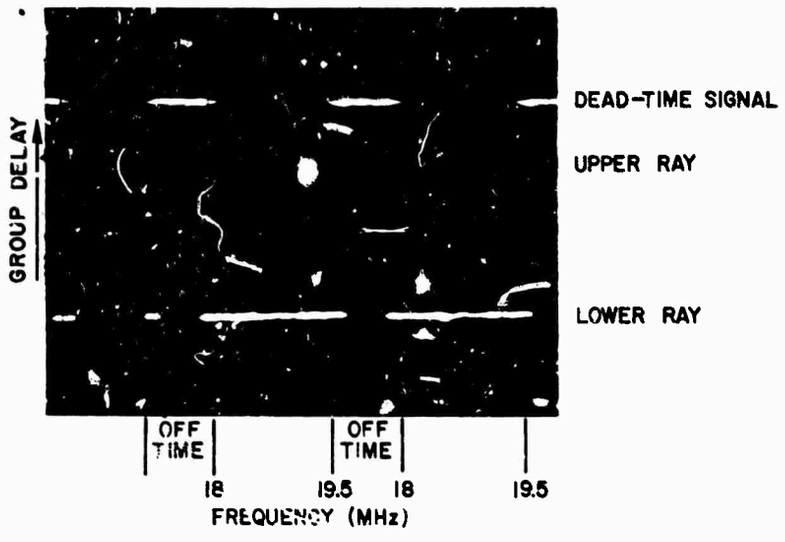

Fig. 24. HIGH-RESOLUTION RECORD OF DATA PRESENTED IN FIG. 22.

observed in this manner corresponds to that predicted from the observed polarization rate: 25 μs at the lower frequency end of the records.

The higher rotation rate observed on the upper ray relative to the lower ray is due to the larger magnetoionic group time differential. The average values of observed polarization rotation rate are of the same order of magnitude as that predicted in Chapter II for F-layer paths.

D. The Effects of Polarization Rotation with Frequency as a Function of Time

In order to understand the effects of polarization rotation with frequency as a function of time, an experiment was performed on 24 and 25 February 1967 utilizing a repetitively swept high-frequency FM-CW sounder. Every half hour a 4 to 30 MHz frequency sweep record was made in order to produce an oblique ionogram. In the time interval between these full sweeps, 4.9 MHz bandwidths were repetitively swept once each 5 sec for 2 min over nearly adjacent portions of the HF band in order to provide a record of the manner in which the amplitude nulls on oblique ionograms move as a function of time. The experimental sequence was repeated throughout the daytime hours. The results presented in Figs. 25 and 26 for 2200-2230 GMT are typical of those observed.

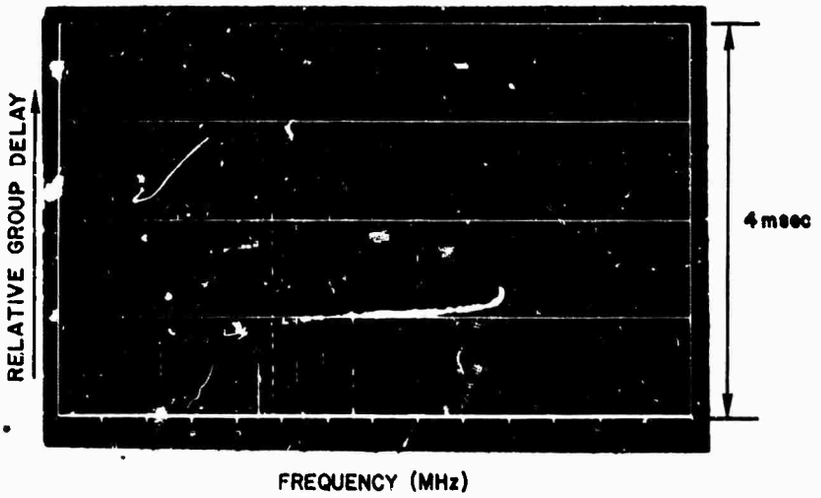

(a) Ionogram

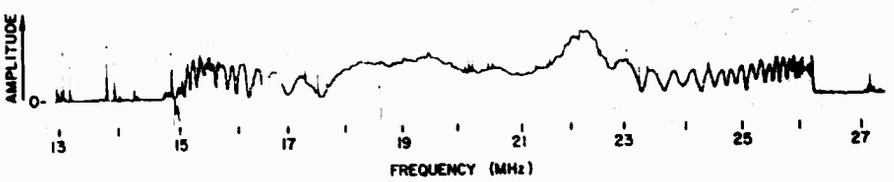

(b) Amplitude vs frequency record

Fig. 25. IONOGRAM AND LOWER-RAY ONE-HOP AMPLITUDE VS FREQUENCY RECORD FOR 2200 GMT ON 25 FEBRUARY 1967.

The ionogram for 2200 GMT and the corresponding diode-detected amplitude vs frequency variations of the one-hop layer ray are shown in Fig. 25. These records are indicative of the nearly constant ionospheric conditions that were present during the half-hour test period. Portions of the one-hop lower-ray repetitive amplitude vs frequency records are shown in Fig. 26 for 16 to 20.9 MHz and for 22 to 26.8 MHz. A sweep was made every 5 sec. Comparison of successive records indicates that amplitude nulls move in the frequency spectrum as a function of time. The records suggest the following:

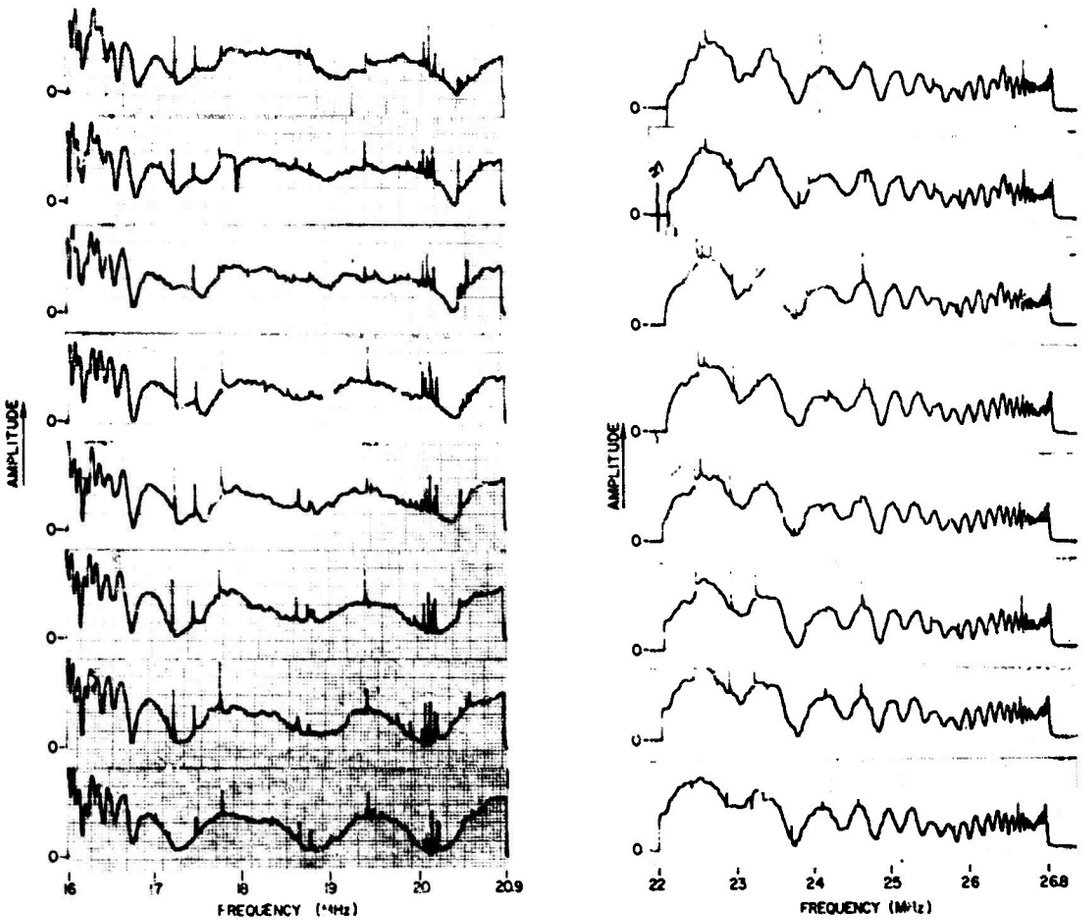

(a) 16-20.9 MHz band (b) 22-26.8 MHz band

Fig. 26. TIME-SEQUENTIAL 5 SEC AMPLITUDE VS FREQUENCY SAMPLES OF THE ONE-HOP LOWER RAY.

1. The amplitude nulls that appear are not as deep as those observed (although at different times) with the log-periodic array because the rhombic receiving antenna was not as truly linearly polarized as the LPA.
2. The amplitude maxima shift in radio frequency as a function of time, but the null-to-null spacings between a given frequency interval remain roughly constant.
3. The nulls shift with time more rapidly at higher frequencies.

An explanation for the apparent motion of the nulls is that their position in the spectrum must change, at any given frequency, in accordance with the effects of polarization rotation with time. A typical measured value for the time required for a change from a null to a maximum at a given frequency was 20 sec. The effects are illustrated in Fig. 27.

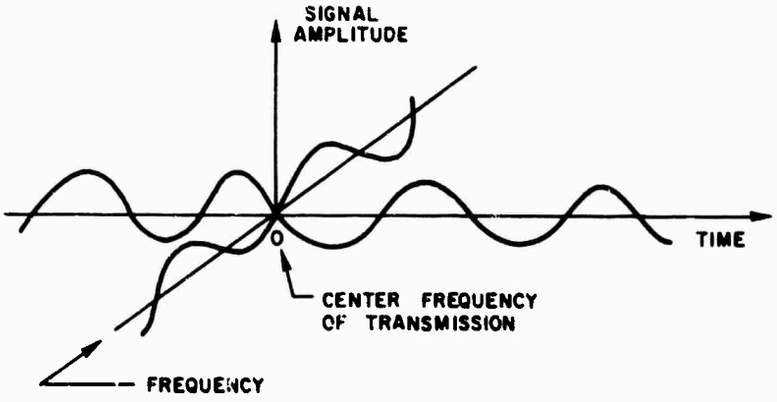

(a) Cross-polarized center frequency

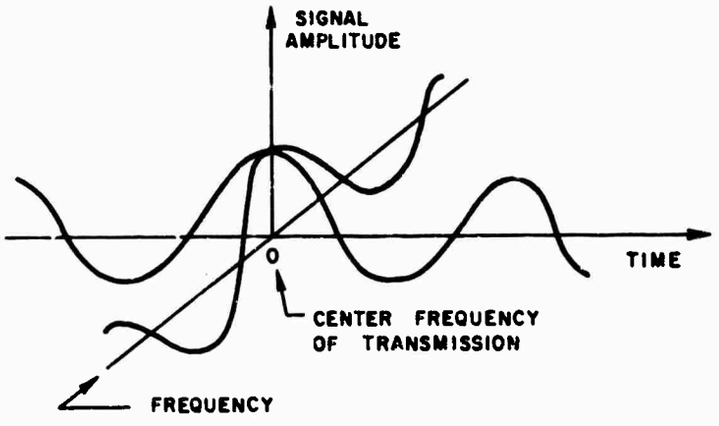

(b) Parallel-polarized center frequency

Fig. 27. EFFECTS OF POLARIZATION ROTATION WITH TIME AND FREQUENCY.

E. Correlation Description of Polarization Phenomena

A measurement technique is presented for determining ionospheric channel amplitude and phase statistics as a function of time and frequency. Knowledge of channel statistics is fundamental to the design of adaptive HF communication systems. In addition to describing the ionospheric

channel signal transfer function, amplitude statistics describe the change of incoming signal polarization. Primary attention is given to the amplitude statistics of the ionospheric channel, although the technique may be employed also to study phase path statistics. Some of the results of this section have appeared previously in Ref. 12.

On 17 December 1966 at approximately 1900 GMT, an FM-CW sweep-frequency HF sounder was swept repetitively at a 1 MHz/s rate over the 16 to 16.5 MHz band as illustrated in Fig. 28. The transmitted signal maintained a constant amplitude and a coherent phase across the spectrum.

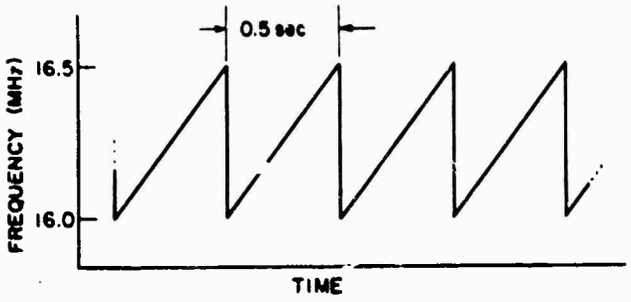

Fig. 28. TRANSMITTED WAVEFORM.

At the time of the experiment, propagation over this range of frequencies was by one-hop mode, as shown in the ionogram in Fig. 21, made a half hour before the experiment.

A strip chart of both the audio signal and its amplitude envelope was recorded for 485 of the half-second sweeps (a total recording time of 4 min, 2-1/2 sec). Part of this record is shown in Fig. 29. The amplitude curves on the charts were manually smoothed, using the full-signal record as a guide, to eliminate the effects of interference bursts that are produced whenever a fixed-frequency radio transmission is swept over. The result of this analysis is a continuous half-second sampling of the amplitude vs frequency characteristic of the ionospheric channel over a 500 kHz band.

The amplitude strip-chart records were sampled 21 times per sweep (including end points) on a Benson Lehner Oscar K machine. This device

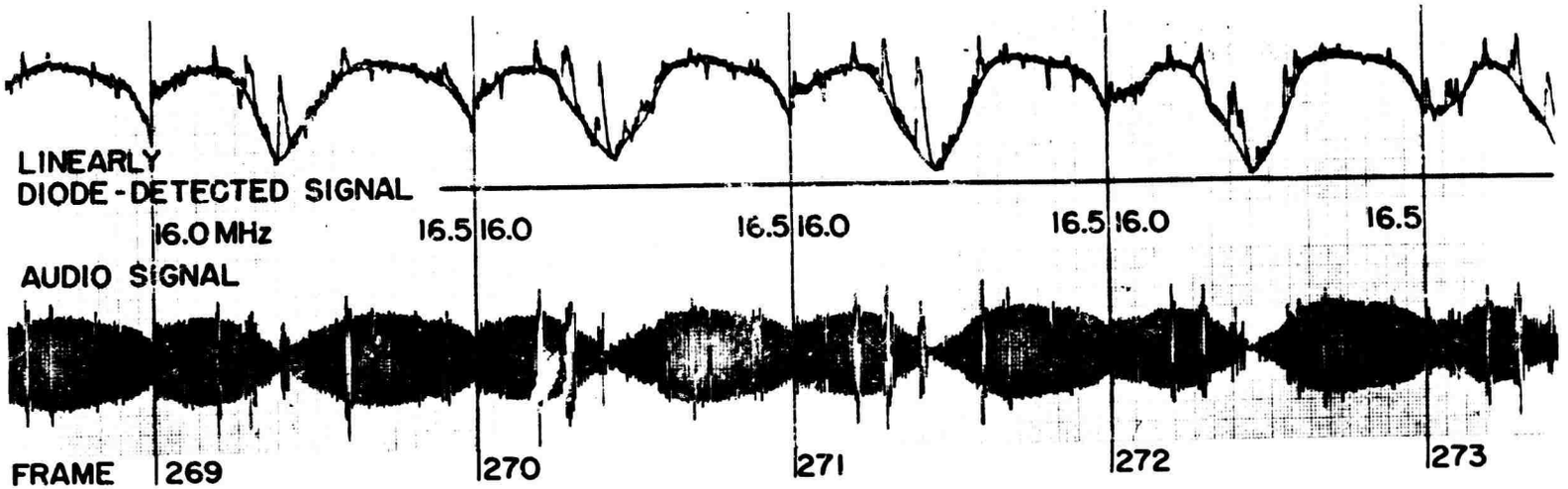

Fig. 29. STRIP-CHART RECORDING OF AMPLITUDE CHARACTERISTICS.

produces punch cards on which the sweep number, sample number, and sample value appear. An IBM 7090 computer was then employed to determine a statistical description of the ionospheric channel. Specifically, plots of average correlation coefficient vs time were made using the full 500 kHz sweep, and 250, 125, and 50 kHz segments of the sweep, by correlating all possible adjacent, alternate, and more widely separated sweeps. A simple correlation average was then determined for each of the possible time spacings. The formulas employed in these computations are presented in Appendix A. The results, shown in Fig. 30, indicate the rapidity with which the amplitude vs frequency characteristic of the ionospheric channel under test changes with time. It can be seen that for all cases considered, the amplitude characteristic decorrelated to approximately 1/e in about 3 sec.

Computations to determine the average autocorrelation coefficient as a function of frequency were made using frequency segments from 50 to 450 kHz. The nature of the autocorrelation function employed (see appendix) is that the largest number of autocorrelation sample values are obtained for the smallest frequency segment. The computer autocorrelated each of the sweeps and then determined a simple average. The results appear in Fig. 31. A "coherent" bandwidth, defined to be the band within which the autocorrelation coefficient is above 1/e, may be determined from the limit of the size of the "1/e bandwidths" as the frequency segments decrease in size. A curve to determine this (shown in Fig. 32) indicates that the coherent amplitude bandwidth at 16.25 MHz was 70 kHz.

The data shown in Figs. 30 and 31 may also be interpreted in terms of average changes in the incoming polarization as a function of time and frequency. Measurements of the distance to the first null of the shorter-segment correlation curves indicate that the incoming polarization of the one-hop lower-ray mode rotates an average of a half-turn once every 10 sec at a given frequency, and once every 100 kHz at a given instant of time.

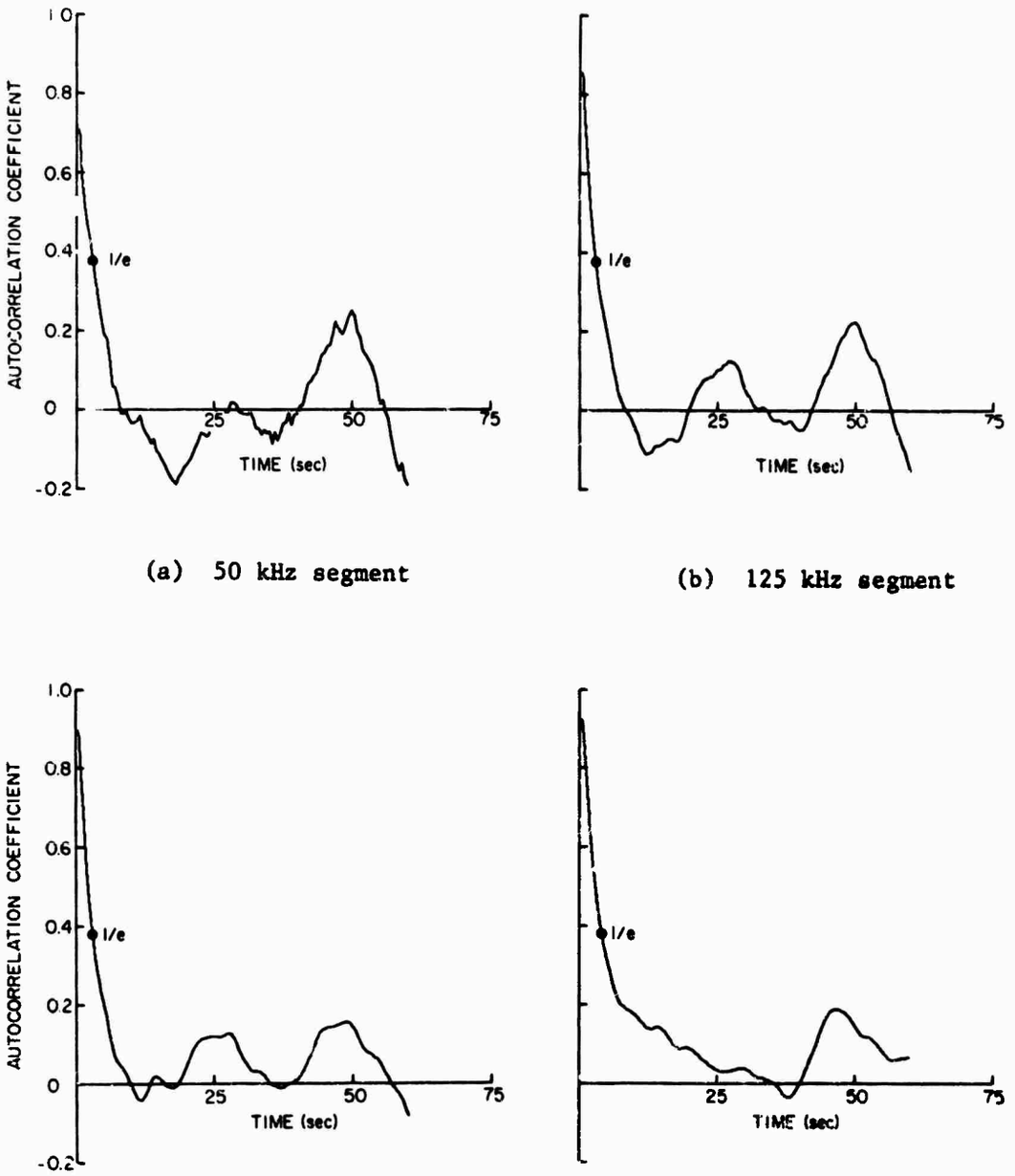

(a) 50 kHz segment

(b) 125 kHz segment

(c) 250 kHz segment

(d) 500 kHz segment

Fig. 30. AMPLITUDE CORRELATION AS A FUNCTION OF TIME.

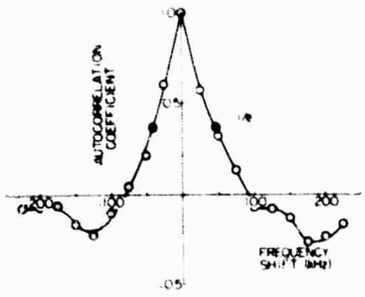

(a) 50 kHz segment

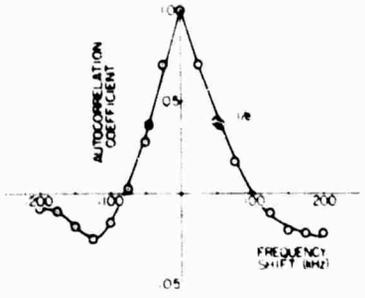

(b) 100 kHz segment

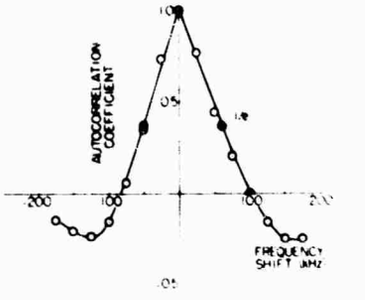

(c) 150 kHz segment

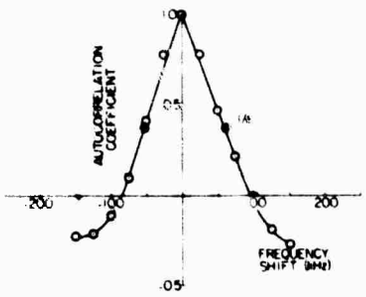

(d) 200 kHz segment

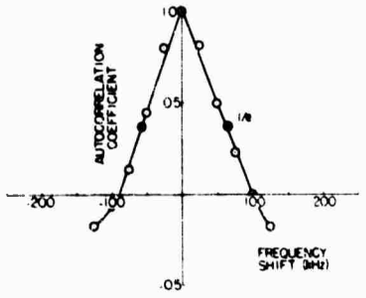

(e) 250 kHz segment

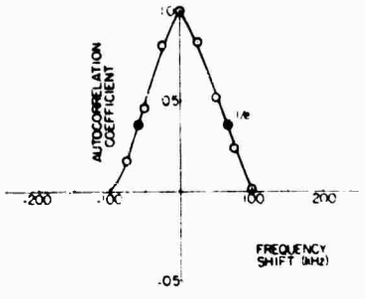

(f) 300 kHz segment

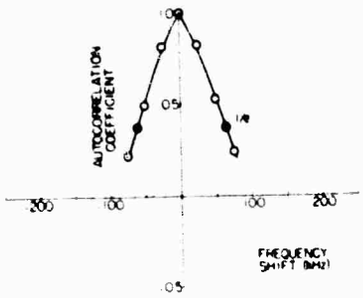

(g) 350 kHz segment

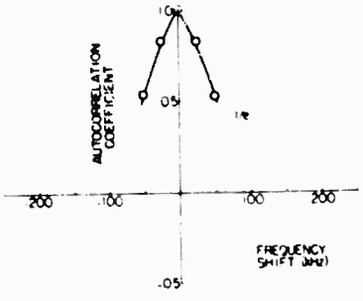

(h) 400 kHz segment

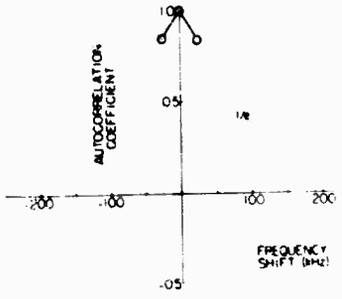

(i) 450 kHz segment

Fig. 31. AMPLITUDE AUTOCORRELATION AS A FUNCTION OF FREQUENCY.

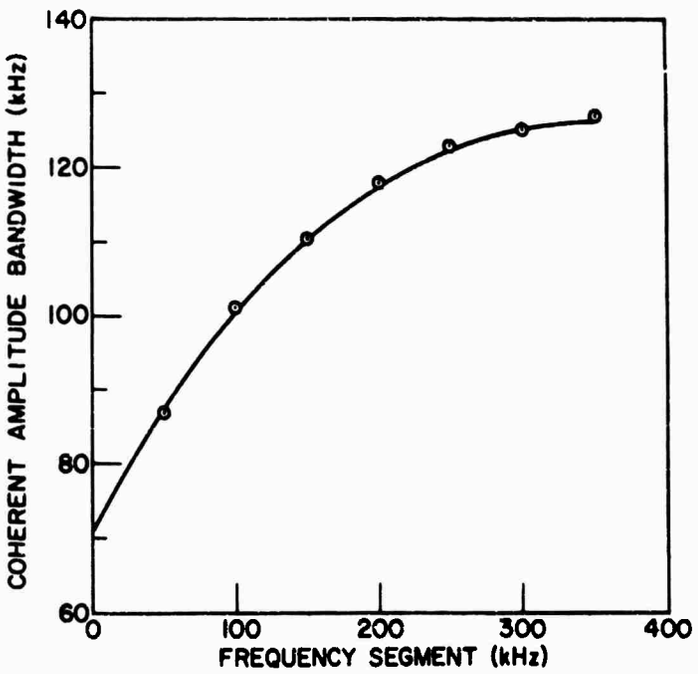

Fig. 32. AMPLITUDE AUTOCORRELATION BANDWIDTH VS FREQUENCY SEGMENT.

BLANK PAGE

Chapter IV

THE EFFECTS OF POLARIZATION ROTATION AND PHASE DELAY WITH FREQUENCY ON OBLIQUE-PATH HF SIGNALS

The effects of ionospheric polarization rotation and phase delay with frequency on HF communications were investigated and the results are presented here. Ionospheric factors affecting skywave propagation are first considered in order to develop a system model for the transmission path. Phase distortion is then considered, including a review of definitions of coherent bandwidths based on phase nonlinearities. A new definition is offered for a coherent bandwidth, called polarization bandwidth, which is a function of the ionospheric polarization rotation rate with frequency. A linear system model for the ionospheric channel, including the effects of both phase and amplitude variations, is proposed from which predictions are made of pulsed signal distortion over ionospheric paths. The concluding sections deal with applications of the results in choosing the polarization of communications antennas to minimize signal distortion, and in adaptively "equalizing" ionospheric channel dispersion.

The relation between signal distortion due to phase effects and measurable ionospheric parameters has been considered previously by various researchers: Budden [3] relates the shape of the group time vs frequency trace on vertical ionograms to channel phase nonlinearities. Sollfrey [13] relates received pulse shape to the magnitude of quadratic phase nonlinearity. Wetzel [14] proposes a coherent bandwidth criterion based on phase nonlinearities, and evaluates it using assumed linear and quadratic electron density profiles (see Section C). Peterson and Vesecky [15] consider the effects of linear and quadratic delay distortion on the shape of short RF pulses. Signal distortion has been discussed as a subject unrelated to physical phenomena by Sunde [16] who considers the effects of linear and quadratic phase distortion on CW signals with various forms of imposed modulation. Rice [17] considers the effects of distortion on FM signals. Signal distortion criteria are defined by Davydov [18] for small nonlinear deviations in amplitude and phase (see Section C).

A. A Model for Signal Propagation in the Ionosphere

A time-invariant linear system is proposed as a model for a slowly varying ionospheric channel which includes the transmitting and receiving antennas. Additive atmospheric noise is neglected, since the noise amplitude is not a function of the amplitude of the transmitted signal--a circumstance that violates the linearity assumption. In addition, the assumptions of time invariance and linearity require that doppler shifts due to ionospheric motions be neglected because such phenomena change the signal component frequencies.

The Fourier theorem states that any wave is equal to the sum of its harmonic components. This implies that a sufficient description for an ionospheric channel is obtained by specifying the change of the amplitude and phase (the two variables necessary for a specification of a Fourier component) experienced by each harmonic wave passing through the channel. Every frequency component at the input appears at the output; and only the zeroth-order derivatives of amplitude and phase are nonzero.

An ionospheric channel of the above form exists for every possible path between transmitter and receiver. Parallel linear channels add, however, so the channel may be thought of as possessing either one transfer function or many transfer functions. It will be found useful in a later section to consider the ionosphere as the sum of two signal transfer functions, one for each of the magnetoionic components. In the following section, however, which deals with signal distortion due to phase nonlinearities, the channel will be assumed to consist of a single ionospheric path. This latter model describes a single mode (e.g., one-hop lower ray) path where intramode multipath is neglected.

B. Determination of Channel Characteristics from Oblique Ionograms

An analytic form for the ionospheric transfer function is here defined in terms of measurable ionospheric parameters. Under the assumptions of Section A, the transfer function of an ionospheric channel may be written as $A(f)\, e^{j\phi(f)}$, where $A(f)$ and $\phi(f)$ are amplitude and phase, respectively. Discussions presented in Chapters II and III indicate that $A(f)$ may be determined from the regular amplitude variations appearing on oblique ionograms. For non-characteristically polarized antennas,

A(f) is nearly completely determined by polarization effects.

The relation between measurable ionospheric parameters and the phase vs frequency transfer function of the ionosphere is well known [3, 13-15]. The phase function $\phi(f)$ is expanded in a Taylor series about the center frequency of transmission. The Taylor coefficients are then related to the frequency derivatives of the time delay vs frequency characteristic that appears on oblique ionograms. If $\phi(f)$ is linear in f, there is no signal distortion but only a time delay equal to $\partial\phi/\partial f$. Thus,

$$\phi(f) = \phi(f_o) + \left.\frac{\partial\phi}{\partial f}\right|_{f_o} (f-f_o) + \frac{1}{2!}\left.\frac{\partial^2\phi}{\partial f^2}\right|_{f_o} (f-f_o)^2 + \ldots$$

is related to the group time delay by use of the relation $\tau(f) = \partial\phi/\partial f$. For smoothly varying $\tau(f)$ functions, only the slope and curvature need be evaluated, as the contributions from higher order terms are small. It can be shown [3] that if the contribution from either the slope or the curvature of $\tau(f)$ is much larger than the other terms, then the series may be written in closed form as a tabulated integral. In summary, by application of the above-described procedure, $\phi(f)$ and A(f) may be determined from an experimentally generated oblique ionogram in order to evaluate the effect on signal shape of phase and polarization variations in the ionospheric channel.

C. Distortion Criteria and Coherent Bandwidths

A new distortion criterion is proposed which relates the level of tolerable signal distortion to measurable ionospheric parameters. The criterion, which is stated in terms of a coherent bandwidth, is evaluated as a function of frequency and azimuth in order to aid in the design of HF communication circuits. Some work concerning signal distortion criteria has been done previously. Davydov [18] argues that small deviations $\Delta A(f)$ from constant A(f) and small nonlinearities $\Delta\phi(f)$ in $\phi(f)$ should be measured not in terms of their absolute values but in terms of the signal transform S(f) by use of the "supplementary" signals:

$$\phi(t) = \frac{1}{\pi} \int_0^\infty S(f)\, \Delta\phi(f) \sin 2\pi ft\, df$$

$$A(t) = \frac{1}{\pi} \int_0^\infty S(f)\, \Delta A(f) \cos 2\pi ft\, df$$

These supplementary signals are the difference between the output and input time functions of a modeled ionospheric path. They are a function of the "error" of the channel and, in fact, are the time functions which describe the additional signal "tails" which appear added onto a pulse after transmission through a dispersive medium. This interpretation has validity only for slight deviations from the nondispersive case. Wetzel [14] extends the above results by defining a percentage distortion factor D,

$$D = 100 \frac{\int_{-\infty}^{\infty} S(f)\, \Delta\phi(f)\, df}{\int_{-\infty}^{\infty} S(f)\, df}$$

which he employs as a measure of path distortion. He shows that when only quadratic or cubic nonlinearity in $\phi(f)$ is present, a simple relation exists between D and the bandwidth W of S(f), where S(f) is assumed to possess a constant amplitude in the frequency domain. That is to say, the expression

$$D = 100 \frac{1}{2W} \int_{-W}^{W} \Delta\phi(f)\, df$$

simplifies into a simple algebraic relation between a single coefficient of the Taylor series of $\phi(f)$ and W, for a predetermined value of D which is set by experience. If the phase nonlinearity is of the form $\alpha(\Delta\omega)^2$ (quadratic nonlinearity), or $\gamma(\Delta\omega)^3$ (cubic nonlinearity), then,

for a value of D of 10 percent, $W = 1.7\,\alpha^{-1/2}$ and $1.9\,\gamma^{-1/3}$, respectively. The above criterion for 10 percent distortion requires that $\alpha = 2.89$ for $W = 1$, or that ϕ varies as $2.89(\Delta\omega)^2 = 104(\Delta f)^2$. Thus, there are many cycles of phase variations across W.

Under quiet ionospheric conditions it has been noted by this author that the shapes of the modes appearing in oblique ionograms remain remarkably constant over periods in the order of tens of minutes. Thus, $\phi(f)$ changes slowly. However, as discussed in Chapter III, A(f) changes continuously as a function of polarization rotation with time. The frequency rate of amplitude nulls (or polarization rotation), however, remains quite constant changing approximately with the rapidity of changes in $\phi(f)$. This suggests defining a channel "coherent" bandwidth in terms of the frequency rate of polarization rotation as a function of frequency rather than in terms of an instantaneous A(f). Since the A(f) function, at least for linearly polarized antennas which are commonly employed in communications today, is predominantly a function of polarization rotation, it seems reasonable to call the amplitude figure of merit the polarization bandwidth. For a general class of signals, the effects of polarization rotation first appear when the incoming polarization varies more than 90° over the signal bandwidth. This is the minimum bandwidth at which a communications link designer might begin to consider the effects of polarization rotation with frequency. Hence we shall define the polarization bandwidth as the signal bandwidth, about a given center frequency, within which the polarization rotates 90°. This angle was chosen over 180°, which is the angle of polarization rotation corresponding to the null-to-null spacings on oblique ionograms, because it was desired to have a bandwidth criterion below which signals could be transmitted without appreciable envelope distortion. The amplitude variations imposed by various definitions of polarization bandwidth are shown in Fig. 33.

Polarization bandwidth can be easily determined from the amplitude nulls appearing on oblique ionograms. Theoretical values of polarization bandwidth as a function of frequency and azimuth are presented in Fig. 34 for the 2000 km one-hop path considered in Chapter II. Polarization bandwidth decreases with increasing frequency and with increased alignment of the raypath along the longitudinal component of the earth's magnetic

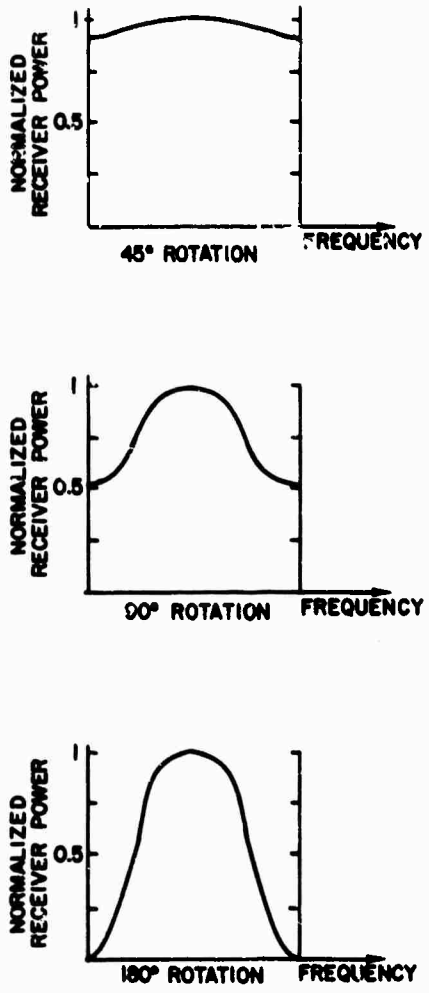

Fig. 33. THE AMPLITUDE VARIATIONS IMPOSED BY THREE POLARIZATION BANDWIDTH CRITERIA.

field. Coherent bandwidths increase from 70 kHz at 17.5 MHz and from 140 kHz at 10.5 MHz, as the propagation direction varies from geomagnetic north to east.

The above definition of polarization bandwidth is supported by some of the results of Chapter II. It is shown there that the frequency rate of change of polarization rotation corresponds to the group time difference between the arrival times of the two magnetoionic components, at least for a QL path. A rate of 1 turn/MHz corresponds to a magnetoionic arrival time differential of 2 μs, and, from above, to a polarization bandwidth of 250 kHz (the approximate bandwidth of a 4 μs gaussian pulse). Thus,

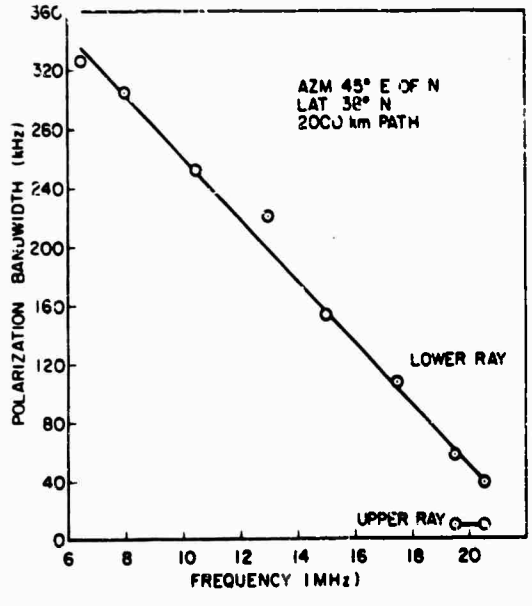

a. As a function of frequency

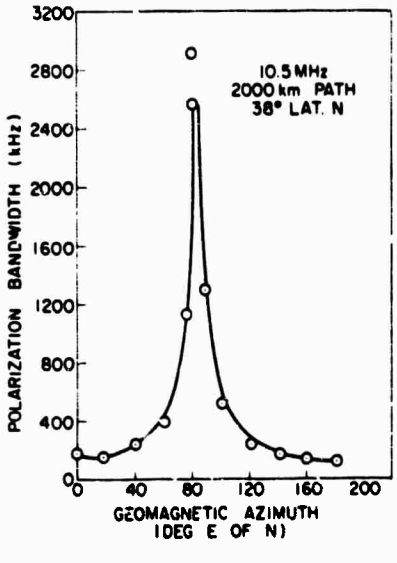

b. As a function of azimuth at 10.5 MHz

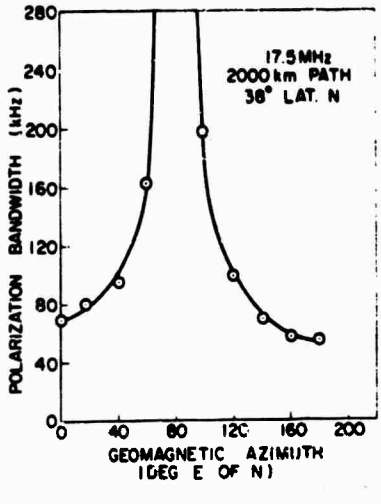

c. As a function of azimuth at 17.5 MHz

Fig. 34. COHERENT POLARIZATION BANDWIDTHS.

after passage through a channel possessing these characteristics, the envelope of the received pulse will appear as one-half the sum of two of

the transmitted pulses possessing a 2 μs relative shift. This is a reasonable boundary criterion for considering the received pulse as distorted.

D. Computer Prediction of Pulse Distortion over Ionospheric Paths

A linear system model is proposed for an ionospheric channel whose parameters are a function of the average phase path and polarization rotation rate. These two parameters may be readily determined from oblique ionograms. The model is employed in predicting the envelope distortion of pulses reflected from the ionosphere under QL conditions and received on a linearly polarized antenna. The discussion will be confined to one-hop propagation.

Consider an ionospheric channel in which the paths of the ordinary and extraordinary rays are treated separately, as shown in Fig. 35a. It

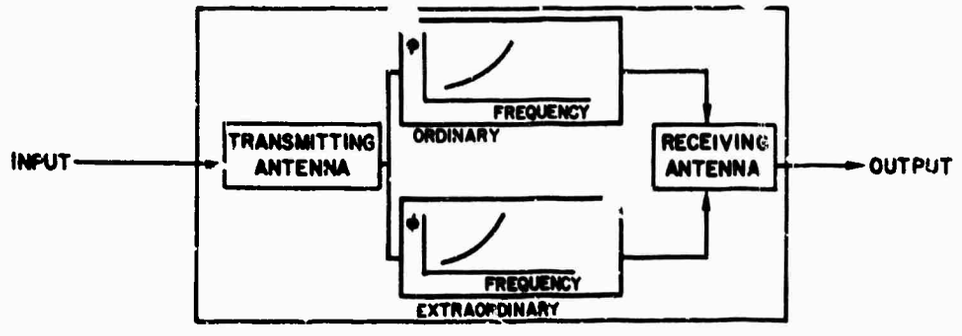

(a) Ionospheric channel model

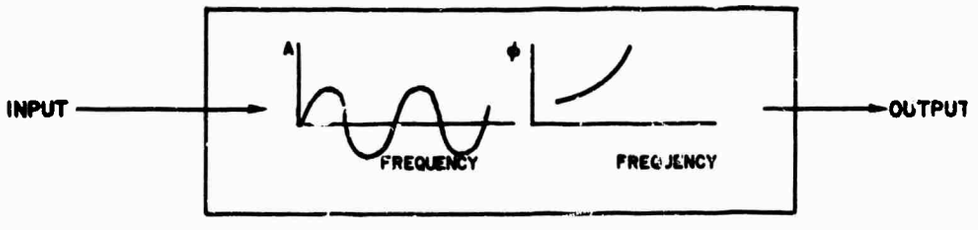

(b) Reduced channel model

Fig. 35. IONOSPHERIC CHANNEL MODELS.

is assumed that the amount of ionospheric absorption is the same for both of the magnetoionic components; hence A(f) is constant for that part of

the channel located between the transmitting and receiving antennas, and only polarization effects determine A(f) for the total path. Under QL conditions the polarization is a function of the difference in the phase paths between the ordinary and extraordinary components. For the purpose of computing changes in signal envelopes after passage over the ionospheric path, the ordinary and extraordinary phase vs frequency characteristics (which are nearly alike) are replaced by the no-field phase vs frequency characteristic. In order to demonstrate the validity of the latter approximation, a Haselgrove equation raytracing program due to Finney [19] was employed with the ionospheric model shown in Fig. 4a to determine phase paths as a function of frequency for the ordinary, extraordinary, and no-field rays over a 2000 km path aligned toward magnetic north (the best situation for differences to become apparent). The results, shown in Fig. 36, indicate that the no-field phase characteristic does not

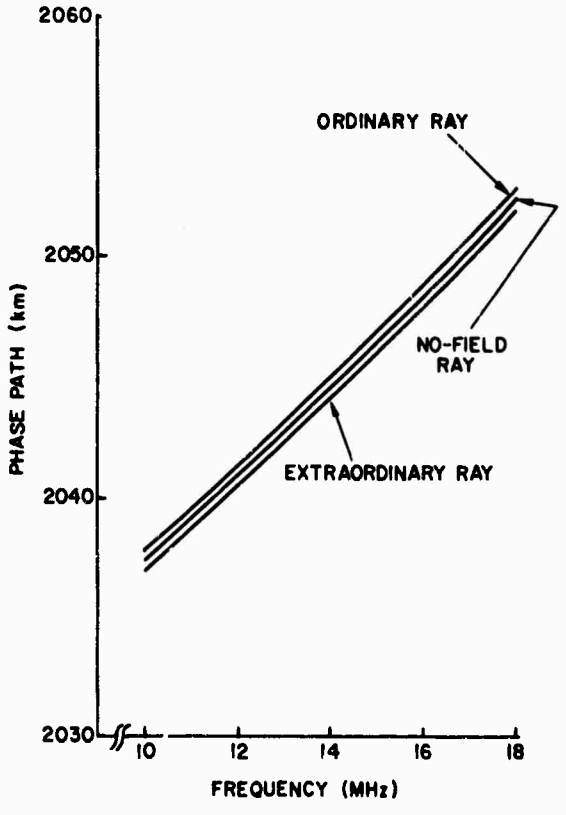

Fig. 36. COMPARISON OF PHASE PATH VS FREQUENCY FOR ORDINARY, EXTRAORDINARY, AND NO-FIELD 2000 KM RAYPATHS.

deviate appreciably from the magnetoionic-component phase characteristics. The no-field phase characteristic may be considered as the "average" phase characteristic for the path. A revised model for the one-hop channel including the above approximations is shown in Fig. 35b. This model takes into account both the amplitude effects due to polarization rotation and the group path differential between the two magnetoionic components, as discussed in Chapter II. The model is valid whether the magnetoionic components arrive separately, overlapped, or coincidently.

The ionospheric transfer function for the model shown in Fig. 35b may be written mathematically as the following Fourier integral, transforming from the frequency domain to the time domain:

$$\text{Output } (t) = \int \text{input } (f) \exp[j2\pi f(t - T(f))] \, A(f) \, df$$

where $T(f) = \phi(f)/2\pi f$. The argument of the integral, input (f), is multiplied by the exponential phase factor $T(f)$ which shifts each of the component frequencies by the appropriate phase time delay. [Input (f) is the transform of the input pulse.] This product is further multiplied by $A(f)$ to describe the effects of polarization rotation with frequency.

In order to evaluate the effect of the variation of signal strength due to the rotation of polarization with frequency, it was necessary to determine the received envelope of short-pulse signals after one-hop ionospheric passage. The ionospheric model included phase time delay vs frequency (Fig. 7), and the amplitude vs frequency due to polarization rotation (Figs. 5 and 6), assuming that signals are received on a linearly polarized antenna. The results (some of which have appeared previously in Ref. 20) were obtained with a digital computer which evaluated the above Fourier integral.

Two cases of polarization-induced distortion are considered. The first assumes that the center frequency of the transmitted pulse coincides with a cross-polarized frequency; the second assumes that the center frequency coincides with a parallel-polarized frequency. The former produces an amplitude null at the center frequency and, in general, produces more

distortion than the latter. Both possibilities are equally likely at an instant of time, as the amplitude at the center frequency varies--with time--according to the effects of polarization rotation with time. The two cases are illustrated in Fig. 27.

Gaussian-shaped RF pulse envelopes of 0.5, 1.5, 5, and 50 μs duration (3 dB width) were considered (Figs. 37 to 43). Figures 37, 38, 40, and

(a) Input

(b) Output, phase distortion only

Fig. 37. ENVELOPE SHAPE OF IONOSPHERICALLY PROPAGATED 50 μs, 17.5 MHz PULSES BEFORE AND AFTER IONOSPHERIC PASSAGE.

41 show these envelope shapes before and after ionospheric phase and amplitude distortion, for a center frequency of 17.5 MHz and for azimuths of 17° and 90°. Data for 0.5 μs pulses with a center frequency of 10.5 MHz are given in Fig. 42.

The time scale indicated for the output pulses in Figs. 37, 38, and 40 to 43 does not include ionospheric transit time. The pulses are symmetric with respect to the ordinate axis because the phase time (not phase) vs frequency characteristic employed in the calculations is linear.

It is important to note that the pulse shapes in Figs. 37, 38, and 40 to 43 represent RF pulse envelopes; compare Fig. 38d and Fig. 39. A zero crossing of any pulse envelope indicates a 180° phase shift in the RF carrier signal.

The 50 μs pulse incurs negligible distortion from the phase and amplitude characteristics, presumably because the 20 kHz pulse bandwidth is less than the 40 kHz polarization bandwidth. The 5 μs pulse is only slightly distorted by the phase vs frequency characteristic, but is

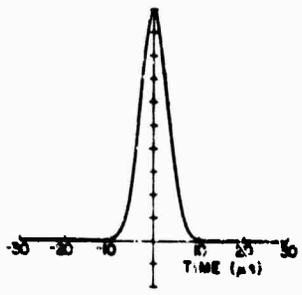

(a) Input

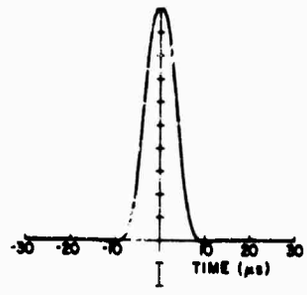

(b) Output, phase distortion only

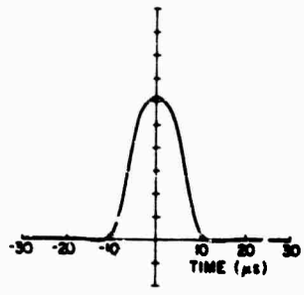

(c) Output, phase distortion and parallel-polarized polarization distortion (17° azimuth)

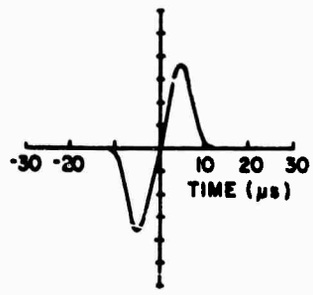

(d) Output, phase distortion and cross-polarized polarization distortion (17° azimuth)

Fig. 38. ENVELOPE SHAPE OF IONOSPHERICALLY PROPAGATED 5 μs, 17.5 MHz PULSES BEFORE AND AFTER IONOSPHERIC PASSAGE.

noticeably further distorted by the amplitude vs frequency characteristic. Phase distortion introduces significant distortion and spreading to about twice the original duration for the 1.5 μs pulse. Either case of polarization rotation with frequency renders the 1.5 μs pulse shape almost unrecognizable and results in a fourfold pulse-duration increase.

The results for the 0.5 μs pulse follow the trend of more severe distortion for larger signal bandwidths. The primary effect of the polarization rotation on the already 20 to 1 time-spread pulse is to further distort the pulse so that it appears as more than one pulse.

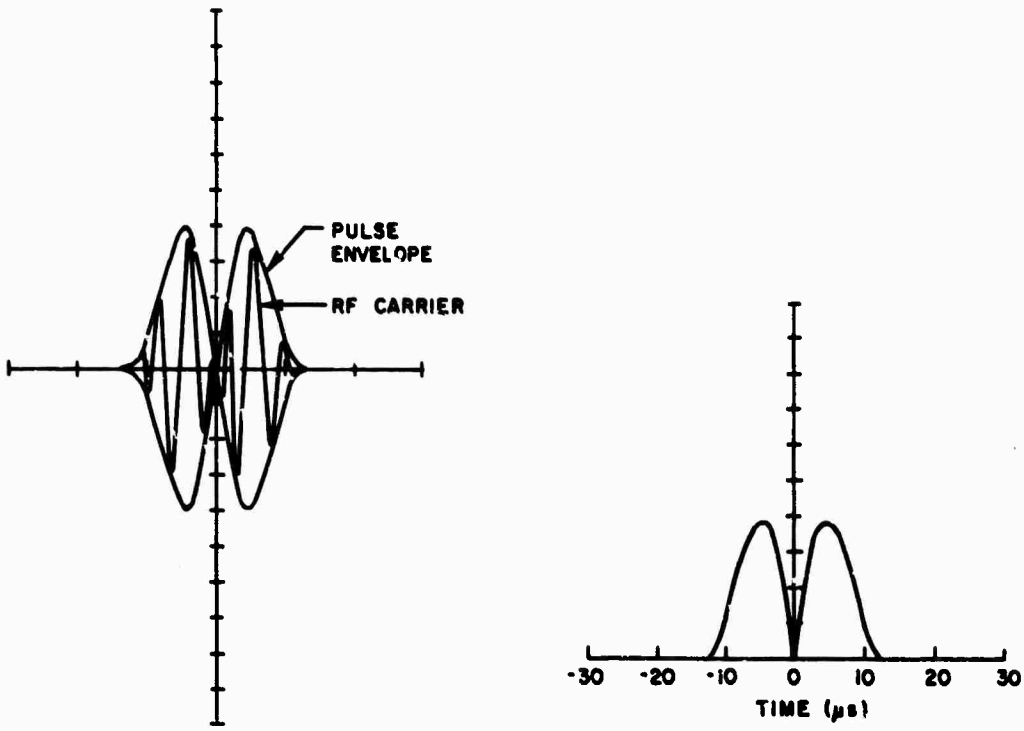

(a) Pulse envelope shape with RF carrier

(b) Diode-detected pulse

Fig. 39. RF PULSE WITH DIODE-DETECTED OUTPUT.

Calculations were also performed to determine the distortion incurred by a 0.5 μs pulse due to polarization rotation over a path with no phase distortion. The results are presented in Fig. 43. The split pulse results from a division of the pulse's spectrum by the amplitude vs frequency characteristic, or equivalently, by the magnetoionic group propagation-time differential, as discussed in Chapters II and III.

Pulse distortion due to polarization effects also occurs for signals propagated over QT paths. When linearly polarized antennas are employed that are <u>not</u> oriented along the QT characteristic polarization directions, or when circularly polarized antennas are employed, variations in the incoming polarization will produce amplitude variations with frequency similar to that discussed above. For the linearly polarized antenna the amount of distortion will be very much a function of its orientation.

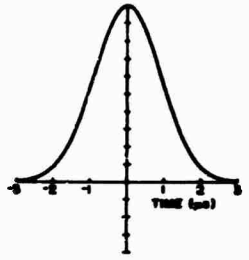

(a) Input

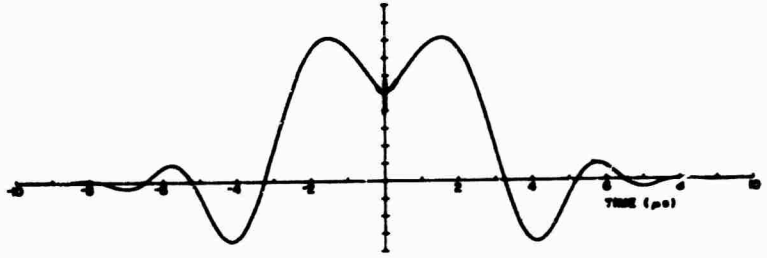

(b) Output, phase distortion only

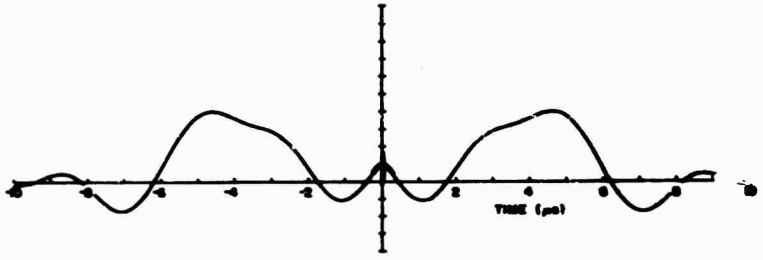

(c) Output, phase distortion and parallel-polarized polarization distortion (17° azimuth)

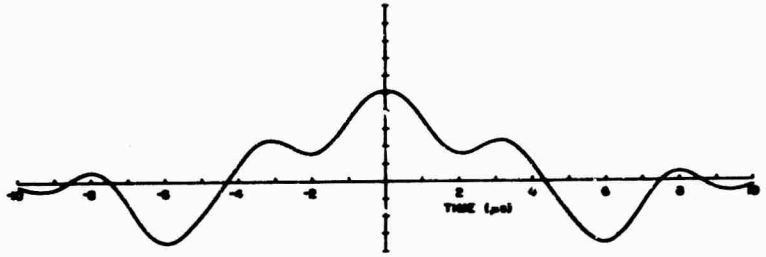

(d) Output, phase distortion and cross-polarized polarization distortion (17° azimuth)

Fig. 40. ENVELOPE SHAPE OF IONOSPHERICALLY PROPAGATED 1.5 μs, 17.5 MHz PULSES BEFORE AND AFTER IONOSPHERIC PASSAGE.

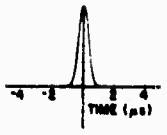

(a) Input

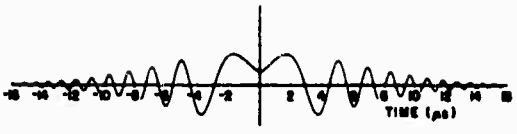

(b) Output, phase distortion

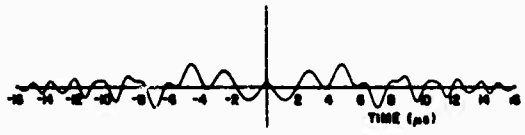

(c) Output, phase distortion and parallel-polarized polarization distortion (17° azimuth)

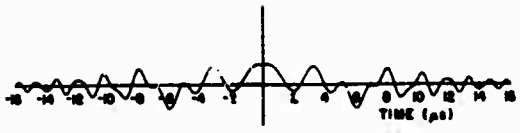

(d) Output, phase distortion and cross-polarized polarization distortion (17° azimuth)

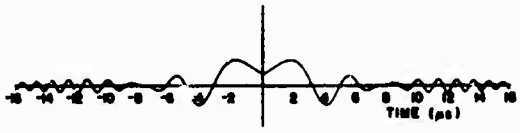

(e) Output, phase distortion and parallel-polarized polarization distortion (90° azimuth)

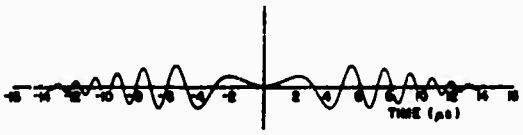

(f) Output, phase distortion and cross-polarized polarization distortion (90° azimuth)

Fig. 41. ENVELOPE SHAPE OF IONOSPHERICALLY PROPAGATED 0.5 μs, 17.5 MHz PULSES BEFORE AND AFTER IONOSPHERIC PASSAGE.

(a) Output, phase distortion

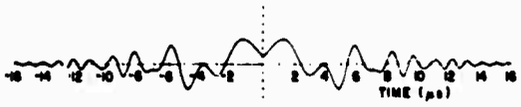

(b) Output, phase distortion and cross-polarized polarization distortion (17° azimuth)

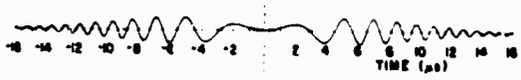

(c) Output, phase distortion and cross-polarized polarization distortion (90° azimuth)

Fig. 42. ENVELOPE SHAPE OF IONOSPHERICALLY PROPAGATED 0.5 μs, 10.5 MHz PULSES AFTER IONOSPHERIC PASSAGE.

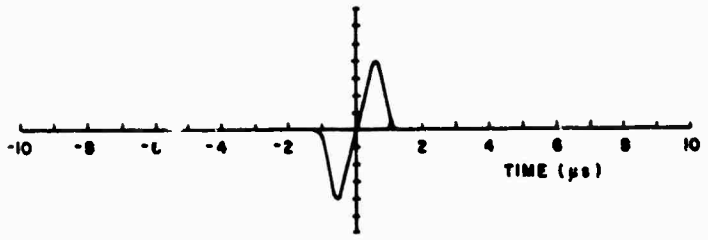

(a) Cross-polarized polarization distortion (90° azimuth)

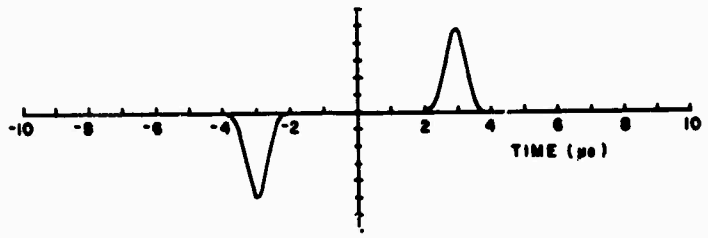

(b) Cross-polarized polarization distortion (17° azimuth)

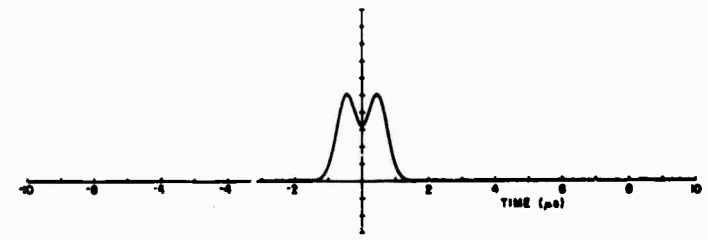

(c) Parallel-polarized polarization distortion (90° azimuth)

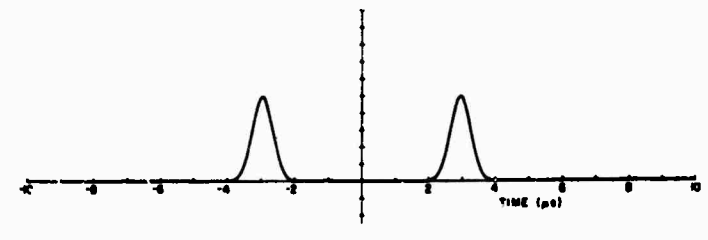

(d) Parallel-polarized polarization distortion (17° azimuth)

Fig. 43. ENVELOPE SHAPE OF IONOSPHERICALLY PROPAGATED 0.5 μs PULSES OVER NO-PHASE-DISTORTION PATHS.

E. Discussion

1. Comparison of Coherent Bandwidth Criteria

The one-hop mode appearing on an ionogram made over the Lubbock-Stanford path will be analyzed in this section to determine the parameters $\phi(f)$ and $A(f)$. From this data the distortion criteria and coherent bandwidth definitions discussed in Section C will be evaluated and compared.

A typical winter-noon ionogram made over the Lubbock-Stanford path is shown in Fig. 13a. A characteristic of these ionograms is that the group time vs frequency variation is nearly linear along the one-hop F lower ray. Measurements made from an enlargement of Fig. 13a indicate that the lower-ray group time delay increases at a rate of 22.3 μs/MHz over the 17 to 26 MHz band; i.e., relative group time may be written as $\partial\tau(f)/\partial f = 22.3$ μs. Thus, the relative phase varies as $\phi(f) = 11.15(\Delta f)^2$ cycles, if f is expressed in megahertz. The amplitude function $A(f)$, described in terms of polarization rotation rate, is shown in Fig. 18 (1951 GMT). Over the 17 to 26 MHz frequency band, the rate is nearly constant at 1 turn/MHz.

The above phase variation may be written in the form used by Wetzel as $0.28(\Delta\omega)^2$. This corresponds to a coherent phase bandwidth W of 3.2 MHz. The amplitude variations due to polarization correspond to a polarization bandwidth of 250 kHz. This value would be smaller for a more magnetically aligned path (see Fig. 34). Thus, at least for the experimental path being considered, polarization effects produce more severe coherent bandwidth requirements than phase path distortion effects. Figures 37 through 43 confirm this relationship.

2. Choice of Antenna Polarization

The discussions of Chapter II indicate that the amount of polarization distortion is primarily a function of the antenna polarization employed. In general, if receiving antenna polarizations corresponding to the limiting ionospheric characteristic polarizations of the path are employed, there are no amplitude effects due to changes in signal polarization; i.e., the phase path variations alone determine the coherent

bandwidth. There are, however, some difficulties associated with the use of characteristically polarized antennas. One problem is that unless the transmitting antenna is also characteristically polarized, there is a loss of signal power due to a "mismatch" between the ionospheric characteristic polarizations and the antenna polarization. For example, for a QL path, linearly polarized transmissions produce equal-amplitude, circularly polarized magnetoionic components. If the receiving antenna was polarized to receive only one of these components, there would be a 3 dB signal loss.

Another problem, as was learned in the course of the experiments described in Chapter III, is that it is difficult to obtain circularly polarized antennas at HF because of ground effects which change the antenna polarization as a function of the vertical angle of arrival of the signal. However, the nearly circularly polarized antennas that were employed, substantially reduced the polarization-induced amplitude changes. This result suggests that it is probably sufficient, for most broadband transmission purposes, to employ antennas that are elliptically polarized-- more improvement being obtained as circularity is approached. If an elliptically polarized antenna is employed such that amplitude minima in the frequency spectrum are one-half of amplitude maxima, much of the polarization-induced signal distortion will be eliminated.

3. "Equalizing" the Ionospheric Path

Since an ionospheric channel may be modeled in terms of amplitude and phase characteristics, it is reasonable to suggest that one could remove these characteristics, or "equalize" the path, by introducing circuits at the transmitter or receiver which approximate the characteristics $A^{-1}(f)$ and $-\phi(f)$. The parameters of these circuits would have to be updated at intervals corresponding to the rapidity of ionospheric changes.

One approach that has been suggested [21] would be to generate equivalent short pulses by the use of FM-CW equipment as described in Chapter III; the frequency rate of the sweep could be varied in accordance with the phase vs frequency characteristic of the ionospheric channel. Another approach* would be to divide the received signal into frequency

*G. Barry, Barry Research, Palo Alto, Calif., private communication.

segments by the use of equally broad, adjacent bandpass filters. Each filter would be followed by a device that could equalize the amplitude and phase. The output signals could then be summed to produce a replica of the transmitted signal. The deviation parameters, which determine circuit characteristics, could be found by sweep-frequency sounding, as described in Chapter III, or by other means. The correlation measurements discussed in that chapter suggest a bandpass filter width of 70 kHz and an updating time of 3 sec. Wider bandpass filters and a longer updating time might be employed if characteristically polarized antennas were also employed.

Chapter V

APPLICATIONS OF POLARIZATION PHENOMENA

A. Communication by Polarization

1. Concepts

Information is normally transferred between skywave communication sites by modulating the radio signal in time or frequency. In this section an additional technique is considered: modulating the signal in space by changing the aspect of the transmitted polarization. It is suggested that the channel capacity may be doubled by the use of antennas that launch characteristically polarized waves. These approaches offer several advantages over conventional techniques.

For a one-hop path, changes in the ionospheric electron density and ordinary internal ionospheric motions result in a variation of the phase path difference between the two circularly polarized wave components with time which produces typical polarization rotation rates of from 2 to 10 turns/min. The relative phase between the extraordinary and ordinary components also varies with frequency (at any instant in time) to produce polarization rotation rates that vary, typically, from 1 turn/MHz to 20 turns/MHz. In the quiet ionosphere, both of the above polarization rates change very slowly. The experimental work of Chapter III has shown that a linearly polarized, east-west transmission results in a linearly polarized wave incident upon the receiving antennas. Thus changes of polarization at the transmitter whose rate of occurrence is rapid compared to natural changes result in closely corresponding changes in polarization at the receiver.

One possible polarization communication system consists of a CW carrier modulated with a key that changes the transmitted polarization from, say, horizontal to vertical as shown in Fig. 44a. The keying will normally be at a rate which appreciably exceeds that of the natural ionospheric polarization rotation rate. If such a signal is received on a linearly polarized antenna, the received signal amplitude will fluctuate

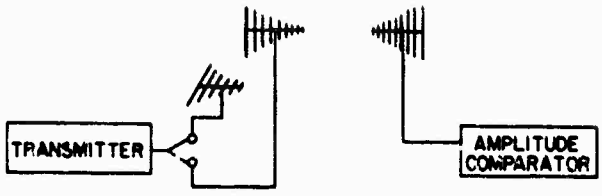

(a) Communication by polarization variation

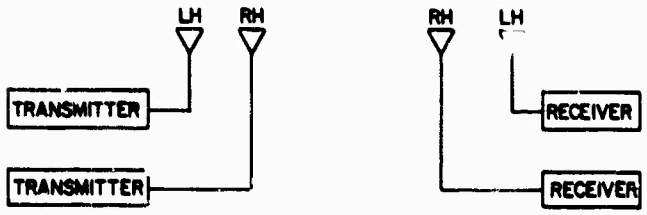

(b) Communication by antennas radiating two characteristic waves at the same frequency (QL case)

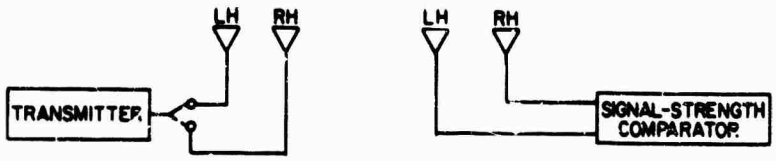

(c) Communication by keying characteristic waves at the same radio frequency (QL case)

Fig. 44. POLARIZATION COMMUNICATIONS SYSTEMS.

in accordance with the transmitter's polarization - and hence keying - although there would occasionally be an ambiguity when the 45°-45° situation occurred.

A better polarization communication technique (shown in Fig. 44b) is to employ characteristically polarized antennas at both ends of the link. Each of the two characteristic wave components will travel through and be reflected from the ionosphere independently. Since the two characteristic waves do not interfere with one another (in the absence of nonlinear effects) each of the characteristic waves may be transmitted at the same frequency but with different modulation, and be separately received and detected at the receiver, thereby doubling the information-carrying capacity of a channel of given bandwidth.

A third example of information transfer by polarization is to switch the transmitted radio signal polarization from one characteristic polarization to the other as shown in Fig. 44c. The signal is received at the receiver on two antennas, each possessing a different characteristic polarization. A comparison is made between the signal strength outputs of the two receiving antennas to determine which characteristic polarization was sent at a given instant of time.

A practical advantage of communicating by polarization is that this technique may be added to existing systems. For example, it may be employed to increase the information-carrying ability of existing on-off keying or FSK systems. In addition to the on-off (or mark-space) information, the user could send another channel of information by keying the sense of the polarization (e.g., from left-hand to right-hand circular polarization). A separate antenna, or a combination of the two characteristically polarized antennas necessary for receiving the polarization-modulated signal, would be employed for receiving the FSK signal. The limiting characteristic ionospheric polarizations for nearly all skywave paths are approximately circularly polarized. One exception is equatorial propagation. Most HF spectrum users currently employ linearly polarized antennas, which would have to be converted to circular polarization by the addition of one new element and a phase-shift network.

Features of communication techniques employing polarization to convey information are:

a. Characteristic polarization modulation may be employed simultaneously with other forms of modulation, thereby providing additional channel capacity to existing systems without recourse to additional transmitting equipment or frequency allocations.

b. Since wave polarization tends to be severely distorted upon ground reflection, communication by polarization is, for practical purposes, limited to one-hop paths.

c. Separate modulation of each of the magnetoionic components at the same radio frequency produces a wave whose bandwidth does not exceed that of the larger of the bandwidths of the two component signals.

2. Experimental Measurements

An experiment was performed to test the feasibility of characteristically polarized communication systems. A 500 W CW signal was transmitted on 22-23 June 1967 from Lubbock, Texas to Stanford, California. The signal was alternately switched from a left-hand to a right-hand circularly polarized transmitting antenna, remaining 6 sec on the former and 4 sec on the latter to guide data interpretation. Chart recordings were made of the signal strengths received on each of two characteristically polarized antennas at the receiving site. The fast AGC outputs of two matched Collins R-390A communication receivers were employed. Experimental arrangements are shown in Fig. 45.

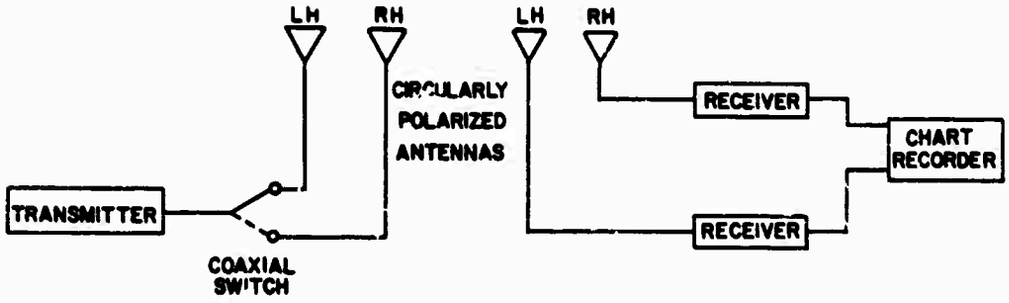

Fig. 45. EXPERIMENTAL ARRANGEMENTS FOR TEST OF COMMUNICATION BY POLARIZATION.

Tests were performed during midday, sunset, and sunrise conditions. All the data, however, regardless of the time of day, exhibited only two classes of results, corresponding to F-layer and interfering F- and E-layer modes as shown in Fig. 46a and b, respectively. The unequally spaced tick marks beneath each recording indicate which polarization was being transmitted, the longer space indicating a left-hand circularly polarized transmission. Left-hand polarized transmissions were best received on the right-hand circularly polarized receiving antenna because of a midpath QT region which reversed the characteristic polarizations of the magnetoionic wave components.

The reason for the effects shown in Fig. 46 may be understood by considering the midday ionogram shown in Fig. 47. Both E- and F-layer modes are visible. The record shown in Fig. 46a occurred approximately

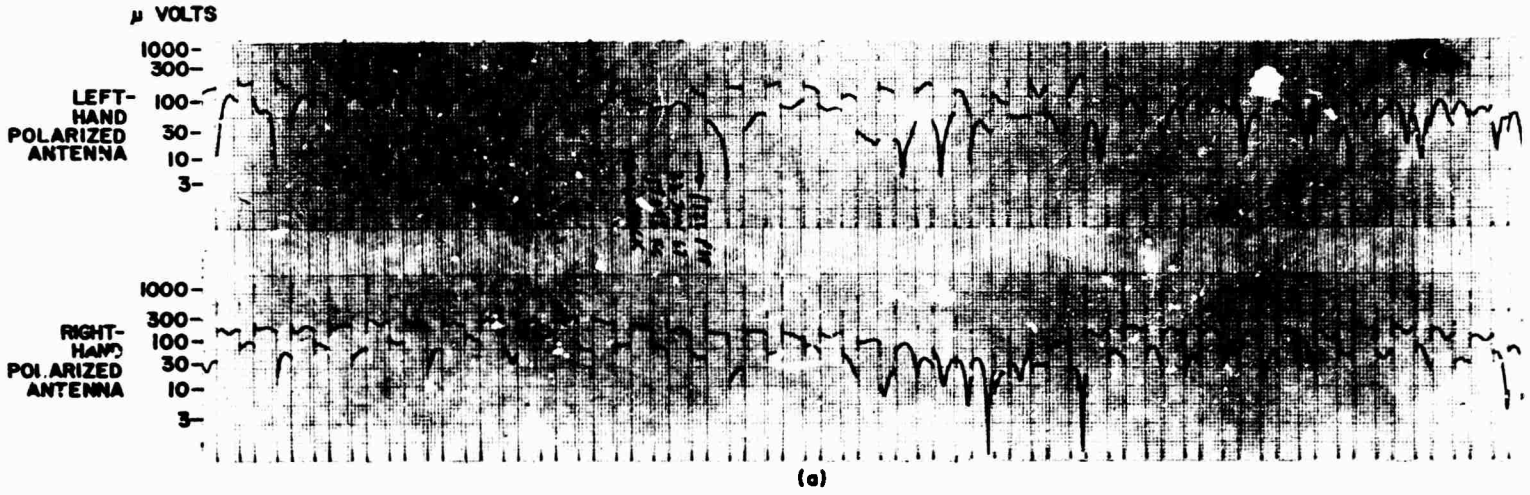

(a) F-layer propagation

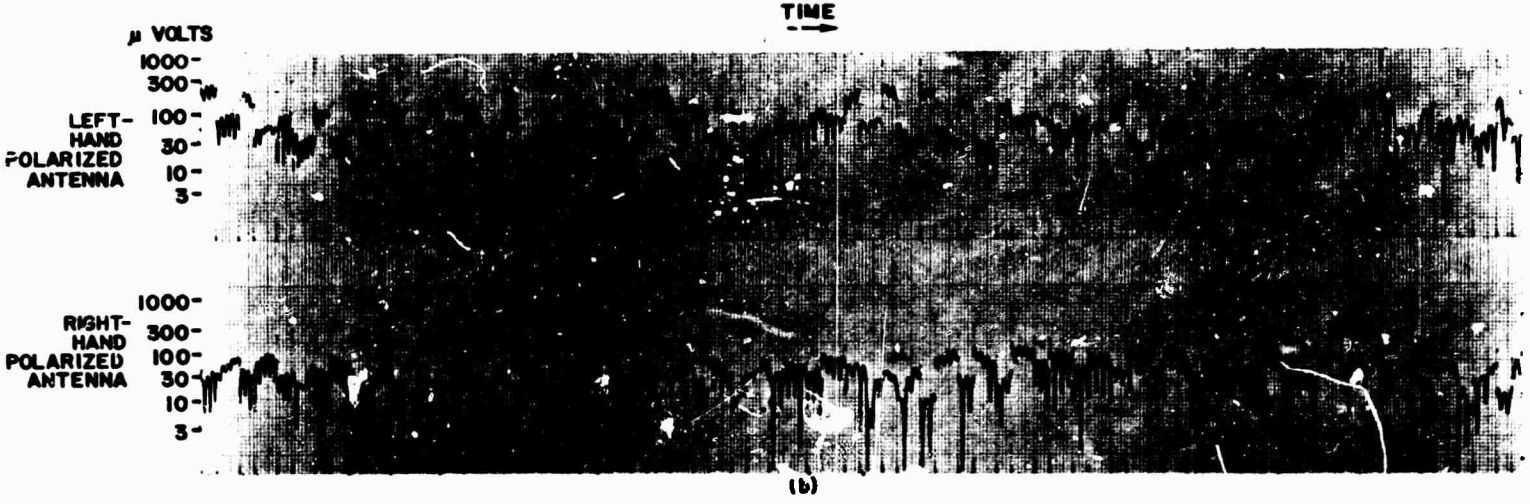

(b) F- and E-layer propagation

Fig. 46. SIGNAL STRENGTHS OF SIGNALS RECEIVED DURING POLARIZATION COMMUNICATIONS TEST.

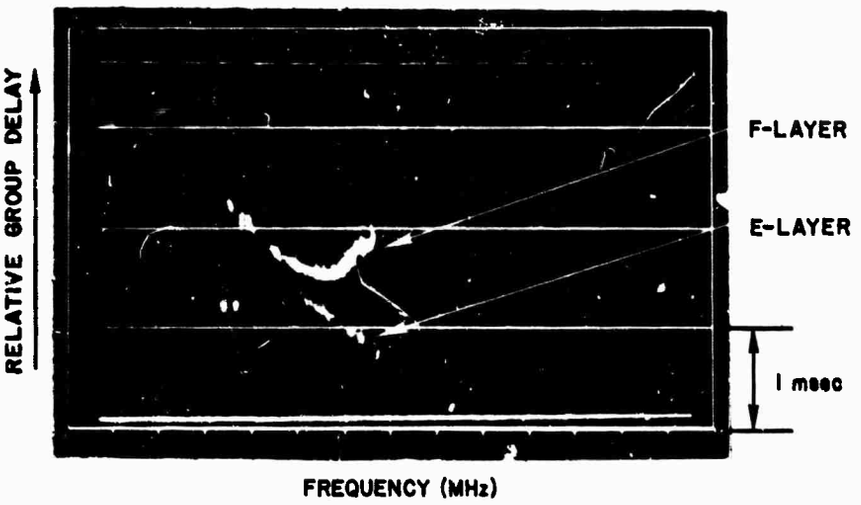

Fig. 47. IONOGRAM MADE DURING MIDDAY TESTS.

70 percent of the time the test was in progress; it probably represents the occurrence of a very weak E-layer propagation path. The 10 to 15 dB signal strength difference exhibited in the single-mode data is approximately equal to the ratio of the signal induced in one antenna due to the presence of a signal on the other antenna. Thus less ionospheric mode cross-coupling could have occurred than is indicated by the above signal strength difference. Under multimode conditions as shown in Fig. 46b, it appears that by careful analysis the transmitted polarization could be determined from the received signal strength data. However, it is expected that under high-rate-of-transmission conditions, the multimode situation would not produce as accurate results as the one-mode situation.

B. <u>The Possibility of Determining Ionospheric Valleys in, and Low-Altitude Values of, the Ionospheric Electron Density Profile</u>

The relation between polarization rotation and group time is employed here to obtain accurate electron density profiles from FM-CW or equivalent oblique ionograms on which the magnetoionic modes are not resolved. The discussion presented is quite brief, the purpose being primarily to cite appropriate literature references.

It has been shown by Storey [22] and Titheridge [23] that by employing both the ordinary and extraordinary rays on vertical incidence ionograms,

one can obtain the size of valleys in the corresponding electron density profile and the values of electron densities below heights corresponding to the lowest sounded altitude. This technique may also be applied, under the assumption of no ionospheric tilts, in determining midpath electron density profiles from oblique ionograms; however, for many paths, oblique sounder resolution does not enable group time separation of the magnetoionic components of the one-hop lower-ray mode. It is under these circumstances that the results of Chapter II-E may be applied.

The first step in obtaining electron density profiles from oblique ionograms possessing amplitude variations due to polarization rotation is to determine two one-hop group time vs frequency graphs corresponding to the two magnetoionic components (Fig. 23). Conversion of each of these graphs to the corresponding vertical ionograms may be performed using Martyn's Equivalent Path Theorem [24]. A preliminary electron density profile may then be obtained by use of Budden's matrix or simplifications of this technique presented by Thomas [25] and Titheridge [26]. Budden's matrix allows for approximate numerical integration, using a finite set of samples, of the integral equation relating ordinary ray virtual to true height. The results of the preliminary calculations are modified, by the use of the difference in group delays between the ordinary and extraordinary traces on the vertical ionogram, to determine the valleys and low-altitude electron density. See Refs. 22, 23, and 27.

C. Registering and Localizing Ionospheric Disturbances by Use of Polarization Techniques

Polarization measurements are employed in this section to determine changes in ionospheric structure. Particular attention is given to the localization of disturbances.

The incoming wave polarization at the receiving antenna after ionospheric reflection is a function of the integrated electron content along the raypath. It is expected, therefore, that changes in the electron density profile, or variations in the raypath, produce corresponding changes in the received polarization as a function of both frequency and time. CW signals received from satellites are regularly employed to determine changes in the integrated electron content of the ionosphere

by the use of polarization techniques (see Little and Lawrence [28]). This method has also been applied by Evans [29] to signals reflected from the moon. The value of the integrated electron content is found by measuring the total number of Faraday turns, by means of two closely spaced CW frequencies, as discussed by Lyon [30].

In general, an ionospheric disturbance (e.g., solar flare) can be viewed as an injection of electrons at a fixed height. A similar model may be employed for traveling disturbances by allowing the height of the increase (or decrease) in electron density to vary as a function of time. For continuously swept frequency sounders a geographically widespread electron injection at a fixed height increases the frequency rate of polarization rotation at frequencies whose height of reflection corresponds to that of the disturbance. This polarization rotation rate increase lasts as long as the increased electron density remains. The group height at the lowest "disturbed" frequency corresponds to the disturbance altitude when a system capable of measuring absolute group propagation time is employed. This effect, which has been observed experimentally, occurs because one of the magnetoionic components is affected by the injected layer before the other. FM-CW oblique ionograms which have been made every 30 sec over a 2000 km path indicate that the observable discontinuity - which travels up or down the one-hop lower ray when traveling disturbances pass through the midpath location - is accompanied by an increased polarization rotation rate with frequency at the "location" of the disturbance.

In the case of a CW signal propagating over the path, an electron injection at a fixed height will increase the rate of amplitude variation due to polarization rotation only while the change in electron density is occurring. One technique that might be employed to localize the disturbance is to transmit two CW signals whose reflecting heights are situated above and below the expected disturbance altitude. A frequency difference of perhaps 1 MHz should give a 10 or 20 km reflecting-height difference for a one-hop path. A disturbance within this height interval will produce a higher rate of amplitude variations due to polarization changes on the higher frequency.

Polarization techniques may also be employed to indicate the presence of field-aligned irregularities. One approach, which may be employed in sweep-frequency backscatter experiments, is to rapidly vary the transmitted polarization and observe at the receiver side frequencies created by the amplitude modulation of the return. The received-signal amplitude varies because the radar cross section of the irregularity is a function of the aspect of the incident wave polarization. The transmitted polarization could be (effectively) rotated by employing two cross-polarized antennas and a motor-driven potentiometer. The polarization rotation rate employed determines the spacing of the resulting side frequencies.

BLANK PAGE

Chapter VI

DISCUSSION AND CONCLUSIONS

A. Theory and Experimental Measurements of Polarization Rotation

The theory of HF ionospheric wave propagation has been shown to predict variations in wave polarization as a function of both the transmitted radio frequency and changes in the ionospheric electron density profile. For a fixed-range skywave path and QL conditions, assuming a linearly polarized transmitting antenna, the wave incident upon the receiving antenna will be linearly polarized, and the plane of the received polarization will rotate with both time and frequency. Computations were performed to determine theoretically the variations in received polarization under QL conditions as a function of frequency and azimuth for a 2000 km Chapman-layer path. The magnitude of the received rate of polarization rotation with frequency was found to increase with increasing radio frequency, path length, and alignment of the propagation path with the longitudinal component of the earth's magnetic field. The polarization rotation rate decreased from approximately 1300°/MHz at 17.5 MHz and from 600°/MHz at 10.5 MHz, as the propagation direction varied from geomagnetic north to east.

A new relation was derived indicating that for one-hop QL paths, the received frequency rate of polarization rotation is a manifestation of twice the group propagation-time difference between the magnetoionic components. This allows a very accurate determination of group propagation-time difference when a low-resolution but continuously swept ionospheric sounder is employed. Such a sounder might be quite unable to resolve, by conventional means, the magnetoionic modes.

Experiments were performed over a period from December 1966 to June 1967, over the 1900 km east-west temperate zone path from Lubbock, Texas to Stanford, California. At the receiving site, two log-periodic arrays rotated 90° with respect to each other were employed to achieve simultaneously both horizontal and vertical reception, as well as both senses of circularly polarized reception. It was found that when a signal strength null appears on one of the linearly polarized antennas, a signal maximum

appears on the orthogonal antenna. A 90° phase difference was observed in the detected outputs of the two linearly polarized antennas. These results provide confirmation of the theoretical predictions that (1) the incoming polarization is linearly polarized, and (2) it is rotating with frequency. It was further observed that the polarization rotation rate first decreased and then increased with frequency along the one-hop lower ray. Theoretically this variation could indicate that the time-delay separation between ordinary and extraordinary rays first decreased as the frequency increased, and then crossed and separated again. The one-hop maximum time delay resolution of an oblique sounder (evaluated in terms of the total time-delay spread of the one-hop lower ray) may be expected to vary similarly. This effect may be due to the presence of lower ionospheric layers not included in the theoretical model. The disappearance of deep amplitude nulls when signals were received on circularly polarized antennas suggests agreement with the theory that antennas possessing characteristic wave polarizations are not subject to the effects of polarization changes. It was found that the upper ray of the one-hop mode also exhibits the effects of polarization rotation but that these associated amplitude variations with frequency occur at a far greater rate than those of the lower ray. This result is expected since the larger magnetoionic group time differential of the upper ray corresponds to a higher polarization rotation rate.

An experiment was performed using a rhombic receiving antenna to determine the manner in which the amplitude effects of polarization rotation with frequency vary as a function of time. The transmitted signal was repetitively swept over 5 MHz bands located throughout the HF spectrum. The records suggest the following:

1. The amplitude nulls that appear are not as deep as those observed with the log-periodic array (although the comparisons were made with data taken at different times) because the rhombic receiving antenna probably is not as perfectly linearly polarized as the log-periodic antenna.

2. The amplitude maxima shift in radio frequency as a function of time, but the null-to-null spacings within a given frequency interval remain roughly constant.

3. The amplitude maxima shift with time more rapidly at higher frequencies.

4. A typical measured value for the time required for a change from a null to a maximum at a given frequency is 20 sec. (The motion of the nulls in the spectrum must be consistent with the amplitude effects of polarization rotation with time, at any given frequency.)

A correlation description of changes of the amplitude vs frequency transfer function of the ionospheric channel as a function of time and frequency was obtained. A computer analysis performed on 16 MHz one-hop lower-ray signals indicated that the amplitude vs frequency characteristic decorrelated to approximately 1/e in 3 sec at a given frequency, and 70 kHz at a given instant of time. The data also indicated that the incoming one-hop polarization rotated an average of a half turn once every 10 sec at a given frequency, and once every 100 kHz at a given instant of time. This experimental technique may be employed in determining design parameters for devices whose purpose is to "equalize" the dispersion of the ionospheric channel.

B. Applications of Ionospheric Polarization Rotation Phenomena

1. The Effects of Polarization Rotation and Phase Delay with Frequency on Oblique-Path HF Signals

A linear model was proposed for signal propagation over ionospheric paths. It was shown that under slowly varying ionospheric conditions, this model can be represented to a good degree of accuracy by an amplitude function $A(f)$ which is a function of polarization rotation with frequency (and antenna polarization), and by a phase function $\phi(f)$ which is the no-field or average phase delay vs frequency. The advantage of this model is that both these parameters may be readily obtained from oblique ionograms where the radio frequency interval between soundings and the bandwidth of the probing signal are sufficiently small. $A(f)$ is obtained from the amplitude null rate with frequency, and $\phi(f)$ is found from the slope and curvature of the group time vs frequency curve.

A measure was proposed for the bandwidth limitation imposed by the effects of polarization rotation with frequency on radio signals transmitted over skywave paths and received on linearly polarized antennas (the predominant type of antenna employed today). This measure, called

polarization bandwidth, is defined as the signal bandwidth across which the incoming signal polarization will vary 90° - the threshold at which polarization effects become apparent in many applications. Polarization bandwidth can be directly related to the frequency rate of polarization rotation.

Computations were performed to determine the polarization bandwidth as a function of frequency and azimuth for a 2000 km Chapman-layer path possessing a maximum usable frequency of 21.5 MHz. The size of the polarization bandwidth was found to decrease with frequency, path length, and alignment of the propagation path with the longitudinal component of the earth's magnetic field. Polarization bandwidths increased from 70 kHz at 17.5 MHz and from 140 kHz at 10.5 MHz as the propagation direction varied from geomagnetic north to east. It was found theoretically that for a 2000 km path, pulses of 50 μs duration transmitted at any azimuth would not be affected by the amplitude vs frequency variations attributed to polarization rotation with frequency. The bandwidth of a pulse of this duration is smaller than the theoretical 40 kHz polarization bandwidth for the path. Pulses of 5 μs duration were affected as a function of azimuth, the amount of distortion being a function of the instantaneous alignment of the incoming polarization with respect to the receiving antenna. The 1.5 μs and 0.5 μs pulses were very distorted in all cases considered.

Comparison was made between theoretical and experimentally determined values of various bandwidth criteria. It was shown that a more severe coherent bandwidth limitation is imposed by amplitude effects due to polarization changes than by phase distortion.

It is suggested that elliptically polarized antennas be employed for high-data-rate communication links. Use of elliptically polarized antennas reduces the depth of the distortion-producing polarization nulls without encountering the design difficulties of constructing HF circularly polarized antennas.

2. Communication by Polarization

It is demonstrated that information may be effectively transferred by polarization modulation over one-hop ionospheric paths. Two possible approaches are considered: polarization variation and the use

of characteristic polarizations. The latter approach, when employed at a single frequency, effectively doubles the information-carrying capacity of the channel. It may be added, for example, to single-frequency telegraphic and FSK systems. An experiment was performed in which the transmitted signal was rapidly switched from one characteristic polarization to the other. The signal was received on a set of characteristically polarized antennas, and the relative signal strengths were compared. It was possible at the receiver to determine the transmitted polarization at all times. This was easier when multipath fading was not in evidence. Features of polarization communications techniques are: (1) The capacity of the channel may be increased without broadening the spectrum, (2) the channel is open only to one-hop paths, and (3) Faraday rotation effects with both time and frequency are eliminated.

3. Determination of Ionospheric Parameters from Polarization Measurements

Techniques exist for making use of both magnetoionic traces appearing on vertical ionograms to determine the size and location of valleys in, and low-altitude values of, the ionospheric electron density profile. These techniques could be applied in determining midpath electron density profiles appearing on FM-CW or equivalent oblique ionograms if the magnetoionic components could be resolved. It is suggested that the relation derived in Chapter II between group propagation time and polarization be employed to obtain two oblique ionograms, corresponding to the two magnetoionic components. Each of these ionograms could be reduced to vertical ionograms for subsequent reduction to an electron density profile.

4. Ionospheric Disturbance Localization

Polarization variations with time indicate changes in the electron density along the raypath, while polarization variations with frequency indicate the value of the integrated electron content. Consider a solar flare that produces an injection of electrons at a fixed height in the ionosphere. The rate of polarization rotation with frequency will increase for all frequencies reflected near the disturbance altitude for as

long as the increased electron density remains. However, the rate of polarization rotation with time for signals reflected from this altitude will increase only during the introduction of the additional electrons. The group height corresponding to the lowest "disturbed" frequency will give the disturbance location. If two frequencies, chosen to reflect at above and below an expected disturbance altitude are employed, the electron injection will produce a difference in amplitude fluctuation rates between the two signals.

Ionospheric phenomena possessing preferred polarization-reflecting properties, e.g., field-aligned electron streams, may be registered by the use of polarization techniques. If both the transmitting and receiving antenna polarizations of a CW backscatter sounder are rapidly rotated in synchronism, then phenomena possessing the preferred polarization property will produce side frequencies in the received signal, which could be detected by aural methods or by spectrum analysis.

C. Suggestions for Further Study

The variation of polarization over skywave paths was here considered as a function of time and frequency. This work can be extended to include the variation of polarization as a function of ground location. The results of such research would be applicable to the design of large antenna arrays. The research may also be extended to include polarization effects over multihop paths. The problem of the wave-ground interaction, which must be considered for multihop paths, has been investigated for forward propagation at HF by Rose [31]. Some related backscatter work has also been reported (Steele [32] and Barnum [33]). The present work could also be extended to other frequency bands.

Appendix A

CORRELATION FORMULAS FOR CHAPTER III

1. Time Correlation

Each of the 485 frames of data consists of 21 points. Thus the i^{th} frame may be written as the set $\{X_{i,j}\}$, $j = 1, \ldots, 21$.

Let

$$\overline{X_{i,a,b}} = \frac{\sum_{j=\lfloor 20(b-1)/a \rfloor+1}^{(20b/a)+1} X_{i,j}}{\frac{20}{a} + 1}$$

and

$$r_{ab}(i,n) = \frac{\sum_{j=\lfloor 20(b-1)/a \rfloor+1}^{(20b/a)+1} (X_{i,j} - \overline{X_{i,a,b}})(X_{i+n,j} - \overline{X_{i+n,a,b}})}{\left[\sum_{j=\lfloor 20(b-1)/a \rfloor+1}^{(20b/a)+1} (X_{i,j} - \overline{X_{i,a,b}})^2 \sum_{k=\lfloor 20(b-1)/a \rfloor+1}^{(20b/a)+1} (X_{i+n,k} - \overline{X_{i+n,a,b}})^2\right]^{1/2}}$$

where the a and b indices are introduced to enable consideration of time segments within a frame: "a" is the number of divisions within a frame and "b" is the order number of each division; n is frame number, or time. Let

$$\overline{r_{ab}(n)} = \frac{\sum_{i=1}^{485-n} r_{ab}(i,n)}{(485-n)\ a}$$

The amplitude correlation vs t... plots are graphs of $\overline{r_{ab}(n)}$ vs n for a = 1, 2, 4, 10 and for b = 1.

2. Frequency Autocorrelation

Let

$$\overline{X_{i,d}} = \frac{\sum_{j=11-d}^{11+d} X_{i,j}}{2d + 1}$$

$$X_{i,d,h} = \frac{\sum_{j=11-d}^{11+d} X_{i,j+h}}{2d + 1}$$

where 2d represents the frequency band about the center sample, and h represents the amount of waveform shift employed in the autocorrelation process. Then, let

$$f_{i,d}(h) = \frac{\sum_{j=11-d}^{11+d} (X_{i,j} - \overline{X_{i,d}})\,(X_{i,j+h} - \overline{X_{i,d,h}})}{\left[\sum_{j=11-d}^{11+d} (X_{i,j} - \overline{X_{i,d}})^2 \sum_{j=11-d}^{11+d} (X_{i,j+h} - \overline{X_{i,d,h}})^2\right]^{1/2}}$$

and

$$f_d(h) = \frac{\sum_{i=1}^{485} f_{i,d}(h)}{485}$$

The plots of amplitude autocorrelation vs frequency are graphs of $f_d(h)$ vs h for d = 1, 2, ..., 9.

REFERENCES

1. Michael Faraday, Experimental Researches in Electricity, vol. III, Bernard Quaritch, London, 1855.

2. Max Born and Emil Wolf, Principles of Optics, Pergamon Press, New York, 1959.

3. K. G. Budden, Radio Waves in the Ionosphere, University Press, Cambridge, 1961.

4. J. A. Ratcliffe, The Magneto-Ionic Theory and Its Applications to the Ionosphere, University Press, Cambridge, 1962.

5. John M. Kelso, Radio Ray Propagation in the Ionosphere, McGraw-Hill Book Company, New York, 1964.

6. K. C. Yeh, "Second-Order Faraday Rotation Formulas," J. Geophys. Res., 65, 8, Aug 1960.

7. T. A. Croft, "Computed Faraday Rotation during Sporadic-E Propagation," Rept. SU-SEL-65-100 (TR No. 113, Contract Nonr-225(64)), Stanford Electronics Laboratories, Stanford, Calif., Oct 1965.

8. T. A. Croft, "Interpreting the Structure of Oblique Ionograms," Rept. SU-SEL-66-010 (TR No. 114, Contract Nonr-225(64)), Stanford Electronics Laboratories, Stanford, Calif., Feb 1966.

9. J. A. Bennett, "The Relation between Group Path and Phase Path," J. Atmos. Terr. Phys., 29, Jul 1967.

10. George A. Dulk, "Faraday Rotation near the Transverse Region of the Ionosphere," J. Geophys. Res., 68, 24, 15 Dec 1963.

11. R. B. Fenwick and G. H. Barry, "HF Measurements Using Extended Chirp-Radar Techniques," Rept. SU-SEL-65-058 (TR No. 103, Contract Nonr-225(64)), Stanford Electronics Laboratories, Stanford, Calif., Jun 1965.

12. M. R. Epstein, "A Statistical Description of an Ionospheric Channel," Rept. SU-SEL-67-078 (TR No. 142, Contract Nonr-225(64)), Stanford Electronics Laboratories, Stanford, Calif., Jul 1967.

13. William Sollfrey, "Effects of Propagation on the High-Frequency Electromagnetic Radiation from Low-Altitude Nuclear Explosions," Proc. IEEE, 53, 12, Dec 1965.

14. Lewis B. Wetzel, "On the Theory of Signal Distortion due to Ionospheric Dispersion," Research Paper P-317, Institute for Defense Analyses, Arlington, Va., Jul 1967.

15. A. Peterson and J. Vesecky, Private Communication.

16. E. D. Sunde, "Pulse Transmission by AM, FM, PM in the Presence of Phase Distortion," Bell Sys. Tech. J., XL, 2, Mar 1961.

17. S. O. Rice, "Distortion Produced in a Noise Modulated FM Signal by Nonlinear Attenuation and Phase Shift," Bell Sys. Tech. J. 38, 4, Jul 1957.

18. G. B. Davydov, "Deviation Tolerances for Phase, Delay, and Attenuation-Frequency Characteristics in Pulse-Signal Communication Channels," Telecommunications and Radio Engineering, 6, Jun 1966.

19. James W. Finney, ESSA, Boulder, Colo., private communication.

20. M. R. Epstein, "Computer Prediction of the Effects of HF Oblique-Path Polarization Rotation with Frequency," Rept. SU-SEL-67-026 (TR No. 139, Contract Nonr-225(64)), Stanford Electronics Laboratories, Stanford, Calif., Feb 1967.

21. D. Belknap, MITRE Corporation, Bedford, Mass., private communication.

22. L. R. O. Storey, "The Joint Use of the Ordinary and Extraordinary Vertical Height Curves in Determining Ionospheric Layer Profiles," J. Res. NBS, 64D, 2, Mar-Apr 1960.

23. J. E. Titheridge, "The Use of the Extraordinary Ray in the Analysis of the Ionospheric Records," J. Atmos. Terr. Phys., 17, 1959.

24. Kenneth Davies, Ionospheric Radio Propagation, National Bureau of Standards Monograph 80, Washington, D.C., 1965.

25. J. O. Thomas, "The Distribution of Electrons in the Ionosphere," Proc. IRE, 47, 2, 1959.

26. J. E. Titheridge, "The Calculation of Real and Virtual Heights of Reflection in the Ionosphere," J. Atmos. Terr. Phys., 17, 1959.

27. A. K. Paul and J. W. Wright, "Some Results of a New Method for Obtaining Ionospheric N(h) Profiles and Their Bearing on the Structure of the Lower F Region," J. Geophys. Res., 68, 19, 1 Oct 1963.

28. C. Gordon Little and Robert S. Lawrence, "The Use of Polarization Fading of Satellite Signals To Study the Electron Content and Irregularities in the Ionosphere," J. Res. NBS, 64D, 4, Jul-Aug 1960.

29. J. V. Evans, "The Electron Content of the Ionosphere," J. Atmos. Terr. Phys., 11, 3/4, 1957.

30. G. F. Lyon, "Some Closely Spaced Frequency Faraday Rotation Satellite Observations," J. Atmos. Terr. Phys., 29, Jul 1967, pp. 871-876.

31. Gerhard Rose, "Determination of D-Layer Absorption along a 2000-km Path Including Endpoints," Stanford Research Institute authorized translation.

32. J. G. Steele, "Backscatter of Radio Waves from the Ground," Rept. SEL-65-064 (TR No. 109), Stanford Electronics Laboratories, Stanford, Calif., Jun 1965.

33. J. R. Barnum, "High-Frequency Backscatter from Terrain with Buildings," Rept. SEL-67-002 (TR No. 130), Stanford Electronics Laboratories, Stanford, Calif., Jan 1967.

UNCLASSIFIED
Security Classification

DOCUMENT CONTROL DATA - R & D

(Security classification of title, body of abstract and indexing annotation must be entered when the overall report is classified)

1 ORIGINATING ACTIVITY (Corporate author) Stanford Electronics Laboratories Stanford University Stanford, California 94303	2a. REPORT SECURITY CLASSIFICATION UNCLASSIFIED 2b. GROUP

3 REPORT TITLE

POLARIZATION OF IONOSPHERICALLY PROPAGATED WAVES

4 DESCRIPTIVE NOTES (Type of report and inclusive dates)

Technical Report

5 AUTHOR(S) (First name, middle initial, last name)

Mark Robert Epstein

6 REPORT DATE October 1967	7a. TOTAL NO OF PAGES 87	7b. NO OF REFS 33
8a. CONTRACT OR GRANT NO Nonr-225(64) b PROJECT NO ARPA 196-67 c. d.	9a ORIGINATOR'S REPORT NUMBER(S) TR No. 143 SU-SEL-67-091 9b. OTHER REPORT NO(S) (Any other numbers that may be assigned this report)	

10 DISTRIBUTION STATEMENT

This document is approved for public release and sale;
its distribution is unlimited.

11 SUPPLEMENTARY NOTES	12. SPONSORING MILITARY ACTIVITY Office of Naval Research Advanced Research Projects Agency

13 ABSTRACT

The theory of wave propagation in the ionosphere, supported by experimental measurements, is used to demonstrate that regular amplitude variations in HF sweep-frequency oblique-ionogram one-hop rays - when linearly polarized receiving antennas are employed - are due to corresponding variations of the received wave polarization with radio frequency. Over quasi-longitudinal paths the rate of occurrence of these variations with frequency (at some instant of time) was found (using computer raytracing techniques) to increase with increasing radio frequency and path length, and with increasingly close alignment of the propagation path with the longitudinal component of the earth's magnetic field. In addition, this rate is shown to be proportional to the group propagation-time difference between the two magnetoionic wave components at a given frequency. This relation explains certain remarkable features of the rate of occurrence of the variations.

Experimental measurements demonstrate that the position in the spectrum of the observed amplitude maxima moves with time in a manner consistent with individual-mode polarization rotation with time at a given frequency. An experimentally determined statistical description of this behavior is obtained for winter-noon conditions.

At some given time, amplitude variations of received signal strength as a function of frequency due to polarization rotation are shown to impose bandwidth limitations on pulsed or broadband skywave transmissions where waveform preservation is important. A measure of this limitation, expressed in terms of a coherent bandwidth, is proposed.

DD FORM 1 NOV 65 1473

UNCLASSIFIED
Security Classification

14 KEY WORDS	LINK A		LINK B		LINK C	
	ROLE	WT	ROLE	WT	ROLE	WT
IONOSPHERIC PROPAGATION						
HF COMMUNICATIONS						
POLARIZATION						

ABSTRACT (Continued)

A model for the one-hop ionospheric signal channel is derived whose parameters are the rate of change of polarization rotation with frequency and the phase vs frequency characteristic of the path. These two parameters are shown to be readily determined from FM-CW or equivalent oblique-path sounding records. Using this model, predictions are made of the effects of polarization rotation with frequency, and also of ionospheric dispersion or phase distortion, on the envelope shape of short-pulse signals. A pronounced waveshape distortion due to the effects of polarization rotation on the pulse envelope was observed when the signal bandwidth appreciably exceeded the "polarization bandwidth" for the path.

A method for skywave communication is proposed which involves polarization modulation and antennas that launch characteristically polarized waves. Experiment shows that this method possesses certain interesting properties not shared by other conventional modulation techniques.

It is proposed that the relation between magnetoionic group time and polarization be applied to FM-CW or equivalent oblique ionograms to determine the size of valleys in, and low-altitude values of, the electron density profile at midpath.

Polarization fluctuations of received ionospherically propagated waves are proposed as potentially useful indicators of the occurrence and location of ionospheric disturbances.